2014

MICROBIAL DIVERSITY AND CONNECTIVITY WITHIN AND BETWEEN OCEANIC AND MARINE SEDIMENTARY COMMUNITIES

Emily Ann Walsh
University of Rhode Island, ewalsh@my.uri.edu

MICROBIAL DIVERSITY AND CONNECTIVITY WITHIN AND BETWEEN OCEANIC AND MARINE SEDIMENTARY COMMUNITIES

BY

EMILY ANN WALSH

A DISSERTATION SUBMITTED IN PARTIAL FULFILLMENT OF THE REQUIREMENTS FOR THE DEGREE OF

DOCTOR OF PHILOSOPHY

IN

OCEANOGRAPHY

UNIVERSITY OF RHODE ISLAND

2014

DOCTOR OF PHILOSOPHY DISSERTATION

OF

EMILY ANN WALSH

APPROVED:

Dissertation Committee:

Major Professor Steven D'Hondt

David Smith

Ying Zhang

Nasser H. Zawia
DEAN OF THE GRADUATE SCHOOL

UNIVERSITY OF RHODE ISLAND
2014

ABSTRACT

Our knowledge of microbial life residing in the oceans- photic and aphotic- and within the subseafloor sediment has grown exponentially within the last few decades. This is partly because of advances in next-generation sequencing technology, which has provided an opportunity to address previously unanswerable questions regarding microbial diversity and biogeography (Hamady & Knight, 2009; Petrosino, Highlander, Luna, Gibbs, & Versalovic, 2009). By utilizing a next-generation sequencing approach, I determined microbial community compositions and assessed their response to environmental and geographic variation within and between five different oceanic regimes (i) the South Pacific Gyre (SPG), (ii) the Eastern and Central Equatorial Pacific (EQP), (iii) the North Pacific Gyre (NPG), (iv) the Bering Sea (U1343), and (v) the Indian Ocean (NGHP-1-14).

My first manuscript, " The bacterial and archaeal biogeography of the deep chlorophyll maximum of the South Pacific Gyre", examines the prokaryotic community composition at a continuous and biologically significant horizon, the deep chlorophyll maximum (DCM), across Earth's largest oceanographic province, the SPG. Our results demonstrate that bacterial and archaeal tag-sequence assemblages of the DCM are strikingly similar throughout the SPG, in terms of the presence and abundance of the most dominant bacterial taxa. Comparison of our SPG bacterial results to samples from the NPG and the relatively nutrient- and chlorophyll-rich EQP shows that DCM assemblages of the SPG, NPG and EQP are statistically distinct from each other, although they have many abundant tags in common. This distinctness is influenced by environmental conditions, as the communities of the two gyres (SPG

and NPG) resemble each other more closely than either resembles the EQP community (which lives geographically between them).

My second manuscript, “Vertical changes in bacterial diversity and community composition from seasurface to subseafloor”, investigates the degree of connectivity between bacterial communities that reside in deep-sea sediment to those that reside throughout the water column at three Pacific Ocean (EQP and NPG) stations. In this study, my collaborators and I investigate a series of ecological gradients through examination into the vertical structure and richness of marine microbes and the how they are influenced by geographic location, light, oxygen concentration and depth. We provide the first pyrosequencing results to (i) address a possible mechanism by which deeply buried sedimentary communities develop deep beneath the seafloor and (ii) assess the degree to which the organisms in those communities are related to communities in the overlying ocean.

My third manuscript, “Bacterial diversity, sediment age and organic respiration in the marine sedimentary environment”, investigates the drivers of microbial diversity and taxonomic richness in deep subseafloor sediment of four geographically distant sites in the Pacific and Indian oceans (U1343, NGHP-1-14, EQP1 and EQP8). To accomplish this goal, my collaborators and I took samples for molecular analysis and interstitial water from a wide range of sediment depths (up to 404 meters below seafloor) and sediment age (up to 5.5 Ma). Our study of these samples demonstrates that abundance-weighted bacterial community composition shifts in response to availability of dissolved metabolic reactants (e.g. oxygen, sulfate, methane). Our study also demonstrates taxonomic richness declines exponentially with sediment age and

generally matches the canonical expectation for changing rates of organic oxidation in subseafloor sediment over time (Jorgensen, 1978; Middelburg, 1989; Westrich & Berner, 1984).

ACKNOWLEDGMENTS

First and foremost, I want to thank my advisor, Steven D'Hondt, for his support, guidance and imparted wisdom shared over the past 5.5 years. I am grateful for all of your insights and training. I would also like to thank my committee: David Smith, Ying Zhang, Tatiana Rynearson and David Rowley for their time, advice and constructive commentary on this work. I would like to thank my fellow co-authors, David Smith, John Kirkpatrick, Rob Pockalny and Mitch Sogin, for their intellectual contributions to these manuscripts. I want to extend a special thanks to Rob Pockalny and Art Spivack for all of their data assistance, presentation advice and dreadful jokes. I owe many thanks to April Parisault and Meredith Clark for their assistance with administrative tasks. A big thanks to my office mates, Justine Sauvage and Mary Dzaugis, and my classmates Rene Olsen and Marion Lytle, for providing countless hours of support both personal and academic. Finally, I would like to thank my parents, my husband and my son, for all of the love and support they have extended to me during my time at GSO.

PREFACE

This dissertation is written in manuscript format and consists of the following three manuscripts: The first manuscript, " The bacterial and archaeal biogeography of the deep chlorophyll maximum of the South Pacific Gyre", examines the prokaryotic community composition at a continuous and biologically significant horizon, the deep chlorophyll maximum, across Earth's largest oceanographic province, the South Pacific Gyre. I gave an abstract and presentation pertaining to this work at a Gordon Research Conference in Barga Italy, July 2012. We submitted this chapter to *Aquatic Microbial Ecology* in June 2014 and we are currently revising it to account for the reviewers' comments. The second manuscript, "Vertical changes in bacterial diversity and community composition from seasurface to subseafloor", examines the vertical structure of marine microbes in seawater and sediment, and how they are influenced by geographic location, light, oxygen concentration and depth. The manuscript then uses this information to address the potential for biological seeding of the deep sediment by the overlying water column. I gave an abstract and presentation pertaining to this research at the American Geophysical Union Fall Meeting in 2010 under the title, "Assessing biogeographic patterns in bacterial community structures from sea surface to subseafloor from three Pacific Ocean stations". My collaborators and I intend to submit this manuscript to the *ISME Journal* to consider for publication. The third manuscript, "Bacterial diversity, sediment age and organic respiration in the marine sedimentary environment", investigates the drivers of subseafloor bacterial diversity and richness from sediment samples taken at four distant and geologically distinct settings including: the Bering Sea (site U1343), the Indian Ocean (NGHP-1-

14), and equatorial Pacific (sites EQP1 and EQP8). I gave an abstract and presentation pertaining to this research at the American Geophysical Union Fall Meeting in 2013 under the title, “Relationship of subseafloor microbial diversity to sediment age and organic carbon content“. My collaborators and I plan to submit this study to *Nature* to consider for publication.

TABLE OF CONTENTS

LIST OF TABLES

LIST OF FIGURES

FIGURE PAGE

INTRODUCTION

Marine microorganisms are highly abundant, extremely diverse and play a significant role in biogeochemical cycles. However, very little is known about their distributional patterns or how they respond to changes in spatial or environmental factors. To address these issues, we sampled microbial communities from the water column and/or sediment at diverse locations, including the Bering Sea (U1343), the Indian Ocean (NGHP-1-14), the South Pacific Gyre (SPG1-SPG10), the North Pacific gyre (EQP11 and Station ALOHA), and the equatorial Pacific (EQP1 and EQP8).

My first chapter , "Bacterial and archaeal biogeography of the deep chlorophyll maximum of the South Pacific Gyre", aims to determine the prokaryotic community composition at a continuous and biologically significant horizon, the deep chlorophyll maximum (DCM), across Earth's largest oceanographic province, the South Pacific Gyre (SPG). Although it has the lowest recorded values of sea-surface chlorophyll on Earth, the size of this open-ocean ecosystem renders it an important contributor to global carbon and nitrogen cycles (Karl et al., 2002; Halm et al., 2011). However, due to a paucity of samples, little is known about the distribution of prokaryotic communities in this oligotrophic environment. To address this issue, we investigate how the microbial community varies along a vast geographic transect, approximating 7,500 kilometers in length, in this most nutrient-limited region of the global ocean. We include samples from the Equatorial Pacific (EQP) and the North Pacific Gyre (NPG) as out-groups to examine if community composition of the DCM varies from region to region or is globally constant within statistically defined parameters. We believe our findings will be of broad interest to the scientific community for the following reasons :(i) the microbiology of the

SPG is largely unknown; (ii) the continuity of DCM bacterial communities throughout the Pacific has been little explored; and (iii) our results shed light on the ocean-scale influence of environmental properties on DCM community composition.

In my second Chapter, "Vertical patterns in microbial community composition and diversity from seasurface to subseafloor", we explore the distribution of bacterial communities along three vertical gradients that range from the seasurface to thirty-four meters below seafloor (mbsf). My collaborators and I sampled these vertical gradients in three geographically and environmentally distinct regions of the Pacific Ocean: the central equatorial Pacific (close to land, high nutrient), the eastern equatorial Pacific (far from land, high nutrient) and the North Pacific Gyre (far from land, low nutrient). Our results demonstrate how microbial communities in these environments are influenced by oceanographic properties, such as chlorophyll content, oxygen concentration, water depth, and sedimentation rate, in both the water column and the sediment below. This sampling strategy also allowed us to assess whether or not the subseafloor bacterial communities at these locations are consistent with "seeding" from the overlying water column. The study is significant to the broader scientific community as: (i) it is the first to explore the relationship between the bacterial communities of deep sediment (>1.5 mbsf) and those of the overlying water column.

My final chapter is titled "Bacterial richness, community composition and organic respiration in the marine sedimentary environment". Rates of metabolic activity (D'Hondt et al. 2002; D'Hondt et al. 2004) and relationships between cell concentration and depth below seafloor (Kallmeyer et al. 2012) suggest that microorganisms buried in the deep subseafloor sediment are under immense selective pressure. However, the

environmental factors that drive this selection still remain unclear. In this study, we used deoxyribonucleic acid diversity data and pore water chemistry of sediment sequences from four distinct geographic locations, including the Bering Sea (U1343), the Indian Ocean (NGHP-1-14) and the eastern and central equatorial Pacific Ocean (EQP1 and EQP8). These data allowed an unprecedented investigation into the environmental factors that influence bacterial diversity and community composition in subseafloor sediment as deep as 404 meters below seafloor (mbsf) and as old as 5.5 million years. In this chapter, we (i) compare how bacterial composition and richness are influenced by the presence or absence of dissolved metabolic reactants (O_2, SO_4, CH_4) and (ii) compare changes in bacterial richness to changes in net rates of organic-fueled respiration (DIC, NH_4) over time. This study is the first to show that microbial diversity decreases with increasing sediment age and the first to link bacterial richness to rates of organic-fueled respiration in subseafloor sediment.

MANUSCRIPT I

BACTERIAL AND ARCHAEAL BIOGEOGRAPHY OF THE DEEP CHLOROPHYLL MAXIMUM IN THE SOUTH PACIFIC GYRE

by

Emily Walsh[1], David C. Smith[1], Mitchell Sogin[2], Steven D'Hondt[1]

[1] Graduate School of Oceanography, University of Rhode Island, Narragansett Bay Campus, 215 South Ferry Road, Narragansett, RI 02882, USA

[2]Josephine Bay Paul Center for Comparative Molecular Biology and Evolution, Marine Biological Laboratory, 7 MBL Street, Woods Hole, MA 02543, USA

Submitted to Aquatic Microbial Ecology June 2014

ABSTRACT

We used 16S rRNA gene tag pyrosequencing to examine the biogeography of bacterial and archaeal community composition in the deep chlorophyll maximum (DCM) of the South Pacific Gyre (SPG), the largest and most oligotrophic region of the world ocean. Bray-Curtis indices show that assemblage composition of these sites is>70% similar for Bacteria and >80% similar for Archaea, although the sites are separated by thousands of km and up to 100 m in water depth. Despite these similarities, communities of the central SPG, the western gyre margin, and the southern gyre margin are distinguishable from each other. Comparison of our bacterial results to samples from the DCM of the North Pacific Gyre (NPG) and the relatively nutrient- and chlorophyll-rich equatorial Pacific (EQP) shows that DCM bacterial assemblage composition is > 50% similar throughout all three regions. Nonetheless, the SPG, NPG and EQP assemblages are statistically distinct from each other, with the communities of the two gyres resembling each other more closely than either resembles the EQP community (which lives geographically between them). Variation in assemblage composition correlates with sea-surface chlorophyll concentration. This study demonstrates that the DCM horizons of different oceanic regions harbor statistically distinct communities that are consistent within regions for thousands of kilometers.

Key words: South Pacific Gyre, microbial biogeography, microbial diversity, deep chlorophyll maximum, pyrosequencing

INTRODUCTION

Oceanic gyres constitute the largest nutrient-limited ecosystems on earth. They encompass 75% of the open ocean, with a total area of 51 x 10^6 km^2 worldwide (Polovina et al. 2008). The largest gyre, the South Pacific Gyre (SPG), lies far from the influence of terrestrial run-off and nutrient rich upwelling zones (D'Hondt et al. 2009). A clear gradient in sea surface chlorophyll (Chl-*a*) that increases from a hyper-oligotrophic center to its oligotrophic edges marks the boundaries of the SPG (Fig.1). The small size of prokaryotes has been inferred to provide a competitive advantage under these nutrient-limited conditions (Dufour et al. 1999).

The hyper-oligotrophic center of the SPG represents the most nutrient-limited region of the global ocean and its deep chlorophyll maximum (DCM) extends to greater depth than anywhere else on the planet (Morel et al. 2007). A permanent feature in both subtropical and tropical environments, DCMs account for a large fraction of net primary productivity in the open ocean (Weston et al. 2005, Huisman et al. 2006). However, little is known about the biogeography and diversity of their resident microbial communities, or how they respond to changes in environmental properties.

The idea that environmental characteristics of a habitat dictate the composition of a microbial assemblage prompts the hotly debated adage, "Everything is Everywhere and the Environment Selects" (Baas-Becking 1934). This theory assumes that microorganisms ubiquitously disperse and microbial distributions are solely explained by habitat preferences (Fenchel & Finlay 2004). Contrary to this belief, recent investigations into historical contingencies, such as evolutionary drift and dispersal limitations, suggest that geographic location may play an active role in determining community structure in various marine and continental environments (Papke et al. 2003, Whitaker et al. 2003, Schauer et al. 2010, Martiny et al. 2011). With this study, we examine how microbial community composition of the DCM varies with geographic distance and environmental properties in the SPG, as well as between the SPG and other major Pacific regions.

To address this objective, we (i) investigated the continuity of microbial assemblages throughout the SPG, and between the SPG and other regions, and (ii) tested how assemblage composition varies with environmental properties, including temperature, dissolved nutrient concentrations, DCM depth and sea-surface Chl-*a* concentration. We sampled the DCM at eight stations along a 7,500 km transect across

the western, central and southern portions of the gyre (Fig. 1). We used samples from the Equatorial Pacific and the North Pacific Gyre as out-groups to examine regional variability within the DCM.

To accomplish our goals, we used massively parallel sequencing (MPS) in marker gene analyses of short, rapidly evolving regions in ribosomal RNA (rRNA) genes. We selected domain-specific primers to target the V6 hypervariable region of the 16S rRNA gene. MPS analyses of these short regions can produce 60-65 bp pyrotags with sufficient taxonomic resolution to assess bacterial and archaeal community diversity (Sogin et al. 2006). These pyrotag data allow us to trace changes in microbial composition throughout Earth's largest oceanographic province.

MATERIALS AND METHODS

Field measurements

We collected our samples during expedition KNOX02RR in southern-hemisphere summer (December 2006/ January 2007) on the R/V Roger Revelle. The samples span a 7,500 km transect through the western, central and southern portions of the gyre (Fig. 1). At each of the eight sites, we cast a CTD-rosette system (Sea-Bird Electronics, Bellevue, WA, USA) and fluorometer (Seapoint, Exeter, NH, USA) and collected water using 10L Niskin Bottles. We used fluorescence to quantify Chl *a* concentrations for all casts except at Station 1. Chl-*a* samples taken for DNA were filtered through sterile polycarbonate membrane filters (0.22 μm pore size GTTP, Millipore) on board and stored at –80°C for shore-based analysis. Nutrient data was analyzed post-cruise using standard methods (Halm et al. 2011). In addition to *in situ* chlorophyll measurements, one-month time averaged sea-surface chlorophyll data were compared to eight day averaged data to

investigate the potential for phytoplankton blooms in the region at the time of sampling (http://disc.sci.gsfc.nasa.gov/giovanni/overview/index.html). No evidence of increased sea-surface chlorophyll was identified for any of the SPG stations.

Pyrosequencing and Community richness

We analyzed 9900 to 32600 bacterial V6-tag sequences and 9200 to 35500 archaeal V6-tag sequences per site, totaling ~178,000 bacterial V6 sequences and ~168,000 archaeal V6-tag sequences for the eight sites according to procedures documented on the Vamps website (vamps.mbl.edu) and in previously published studies (Sogin et al. 2006, Huber et al. 2007, Huse et al. 2007, Huse et al. 2010). We used the Global Alignment for Sequence Taxonomy (GAST) algorithm to assign taxonomy to the tag sequences using a reference database of rRNA genes based on the SILVA database (Huse et al. 2008). To avoid bias introduced during the filtering and clustering process, we clustered all of the analyzed V6 sequencing data according to the single linkage pre-clustering (SLP) method (Huse et al. 2010).

We compared our SPG data to bacterial data from the deep chlorophyll maximum (DCM) of two distinct oceanographic regimes, the North Pacific Gyre (NPG) and the Equatorial Pacific upwelling zone (EQP). The NPG data are publicly available data from three samples of the Hawaiian Ocean Time-series (HOT, 22° 45'N, 158° 00'W), taken at three time points throughout 2006 and 2007(August-HOT 186, October-HOT 189 and February-HOT 194) (http://hahana.soest.hawaii.edu/hot/). These three samples provide a broad perspective on the influence of seasonality at this horizon in this region. We collected the EQP samples during *R/V Knorr* 195 (III) expedition in northern hemisphere

winter (January 2009); they are separated from each other by nearly 60 degrees of longitude (Station 1: 1°48.21' N, 86°11.29' W; Station 8:0°00.36' N, 147°47.50' W).

We amplified DNA extracts using PFU turbo polymerase (Stratagene, La Jolla, CA) in combination with 1x PFU reaction buffer, 200 μM dNTPs, 0.2 μM of selected forward and reverse primers. The primers for the NPG and SPG samples target conserved sequences that flank the V6 hypervariable region. The forward bacterial v6 primer 967F included an equal mixture of the following degenerate variations: CTAACCGANGAACCTYACC, CNACGCGAAGAACCTTANC, CAACGCGMARAACCTTACC, ATACGCGARGAACCTTACC. The reverse bacterial v6 primer 1067R included an equal proportion of the following: CGACAGCCATGCANCACCT, CGACAACCATGCANCACCT, CGACGGCCATGCANCACCT, CGACGACCATGCANCACCT. Archaeal samples were amplified using archaeal forward primer 958F (AATTGGANTCAACGCCGG) and archaeal reverse primers 1048R major and minor (CGRCGGCCATGCACCWC, CGRCRGCCATGYACCWC). For the EQP samples, we amplified a longer rRNA region that included the V4 thru V6 region defined by the 5' primer 518F (CCAGCAGCYGCGGTAAN) and the 3' primer 1064R (CGACRRCCATGCANCACCT) that amplified the NPG and SPG samples.

We used the same thermocycling conditions (94°C for 3 min, 30 cycles of 94°C for 30 s, 57°C for 45 s and 72°C for 1 min, and a final 72°C extension step for 2 min) for all samples analyzed in this study. We pooled PCR products prior to clean-up on a MinElute PCR purification column (Qiagen, Valencia, CA). We analyzed all samples were analyzed on the same sequencer at MBL. To correct for the differences in read

length, we trimmed the EQP sequences to match those of the NPG and SPG stations and re-entered into the GAST system for sequence identification. We could not find DCM archaeal datasets for either the EQP or NPG locations. Consequently, we did not include archaeal data in our comparison of SPG microbial communities to communities from other regions.

Accession numbers and data availability

The sequencing results and supporting data are publicly available on the VAMPS website (http://vamps.mbl.edu) under the following project ID: SPG (KCK_KNX_Bv6, KCK_KNX_Av6), EQP (KCK_EQP_Bv6_CUT) and NPG (KCK_HOT_Bv6). The VAMPS site also provides project metadata including information about sampling conditions and environmental factors.

Statistical Analyses

We performed statistical analysis with the Primer-e and vegan software packages (Clarke & Gorley 2006, Oksansen et al. 2011) on all samples, in order to examine relationships between environmental variables and microbial community composition. We performed non-metric multidimensional scaling plots (nMDS), agglomerative hierarchical clustering algorithm (CLUSTER, group-average), similarity profiles (SIMPROF), analysis of similarity (ANOSIM), spearman rank correlations (RELATE), similarity percentages (SIMPER), Envfit test and bioenvironmental statistical test (BIOENV) on species data sets. We generated resemblance matrices using Bray-Curtis similarities for biological data and normalized environmental data into Euclidean distance for the BIOENV test. We performed rarefaction analysis using the SLP generated clusters at 3% dissimilarity.

RESULTS

Environmental properties of the SPG, EQP and NPG

The DCM varies from 100 to 200 meters below the sea surface throughout the SPG, with its greatest depth occurring in the heart of the gyre (Station 7). The DCM represents a maximum in chlorophyll concentration; due to photo-acclimation, it is not necessarily a maximum in biomass. The DCM is much shallower at the western edge (Stations 1 and 2) and southern edge of the gyre (Station 9 and 10) (Table 1). Despite being shallower at the western and southern edges, the DCM formed well below the depth of the pycnocline at every sampled SPG station (Fig. S2). The temperature of the sampled horizon varied from 11°C at the southern gyre edge to 20°C along our northern sample transect. Salinity ranged from 34.3 to 35.6 psu and *in-situ* chlorophyll-a concentration ranged from 0.22 to 0.40 mg/m^3 (Halm et al. 2011). Average annual sea surface Chl-*a* concentrations (mean SeaWiFS data from September 1994-December 2004) at each site range from 0.029 to 0.117 mg/m^3, with the lowest values in the central gyre (Station 7) (Behrenfeld & Falkowski 1997, Gregg et al. 2005). This ultra-oligotrophic status agrees with a complementary study that revealed concentrations of dissolved phosphate and nitrogen remained below detection limits from the sea surface to about 100 meters below the sea surface at Stations 1-7 (Halm et al. 2011). To consider the possibility that blooms affected our data, we examined satellite chl data for the eight-day and one-month windows that preceded our sampling date at each site (http://disc.sci.gsfc.nasa.gov/giovanni/overview/index.html). There is no evidence of a bloom preceding our sampling at any site (data not shown).

The sampling sites outside the SPG varied significantly in their sea-surface chlorophyll content, ranging from 0.87 to 1.18 mg/m^3 in the EQP to 0.082 mg/m^3at Station Aloha in the NPG (Behrenfeld & Falkowski 1997, Gregg et al. 2005). While the DCM was relatively deep in the NPG (100 m), it was shallow in the eastern equatorial Pacific (41 m at Station 1, 34 m at Station 8 (Walsh et. al. Unpublished). All DCM samples from the NPG as well as the sample from EQP 1, resided below the pycnocline; while the DCM of EQP 8 resided above (Fig. S2). Sea surface temperature (SST) remained between 22.67 °C and 23.63°C at Station Aloha (http://hahana.soest.hawaii.edu/hot/; (Karl & Lukas 1996)) during the 2006-2007 timeframe. At the time of sample collection, sea-surface temperature was 17.45 ˚C at EQP Station 1 and 24.27˚C at EQP Station 8.

Community Composition of the SPG

For all SPG sites, the Global Alignment for Sequence Taxonomy (GAST) algorithm (Huse et al., 2008) showed that the most abundant bacterial pyrotags represented Alphaproteobacteria, Gammaproteobacteria, Bacteroidetes, Cyanobacteria and Deferribacteres (Fig. 2 (major family contribution of these classes)). A majority of the archaeal sequences (95-99%) at each site showed best matches to Marine Group II (MGII) (~64%) and Marine Group III (MGIII) (~34%) Euryarchaeotes. Alphaproteobacteria comprised the most abundant bacterial group at each station and was relatively more abundant in the central and southern portions of the gyre. Gammaproteobacteria composed the second most abundant bacterial group at each station, except at Station 1, which contained the highest proportion of Cyanobacteria in the gyre. While a high percentage of Cyanobacterial tags occurred at every station, their

relative abundance diminished along the path of the SPG transect (from western gyre edge to gyre center to southern gyre edge). In contrast, the proportion of Firmicutes did not substantially change in the western and central portions of the gyre, but increased in the southern region of the gyre (Stations 9 and 10). Other dominant groups such as Bacteroidetes, Deltaproteobacteria and Actinobacteria did not show variation in their relative abundance from station to station (Fig. 2).

The most common bacterial tag at each station matches *Pelagibacter ubique* of the SAR 11 clade, which comprises 57 % of the total identified Alphaproteobacterial tags and 16.3% of all identified bacterial tags. Tags from the SAR 11 clade collectively comprise 76.5 % of the Alphaproteobacterial tags and 21.9% of all the identified bacterial tags in all of our samples. Tags attributed to Rhodobacteraceae and Rhodospirillaceae round out the Alphaproteobacteria, comprising 2.4 and 4.2% of the bacterial tags, respectively. The most abundant representatives of the Gammaproteobacterial group include SAR 86 (9.9%), *Alteromonas* (2.4%), *Halomonas* (1.4%) and an unknown Gammaproteobacteria species (1.4%). Bacteroidetes tags constitute 12% of the total identified tags in our SPG samples; they include unknown Flavobacteriaceae (6%), *Owenweeksia* (2.1%), Marinoscillum (1.9%), and Cryomorphaceae unknown (1.3%). Cyanobacterial tags (11.9%) were all identified as *Prochlorococcus*. The *Defferibacter*tags (9.2%) all align to the SAR 406 clade.

The archaeal tags display far less taxonomic diversity. MGII dominates the archaeal community, comprising 64% of the archaeal tags. MGIII constitutes 34% of the total archaeal tags. Marine Group I (MGI) and Halobacteriaceae each comprise less than one percent of the total archaeal tags.

Diversity within the SPG DCM

Abundance-weighted (Bray-Curtis) diversity indices indicate that the composition of relatively abundant taxa in the DCM remains strikingly similar throughout the SPG. In contrast, the Jaccard index (presence/absence) differs greatly from sample to sample, indicating that rare taxa differ greatly from sample to sample (Boyle et al. 1990) (Fig. 3). Although bacterial diversity is high, the long-tailed rank abundance curve for each sample, along with the Jaccard results, suggests that very low abundance taxa account for most of the bacterial diversity (Fig. S1).

Taxon-independent analyses using SLP clustering reveal that the diversity of bacterial OTUs (≤ 97% similarity) exceeds diversity of archaeal OTUs at all eight sites. Rarefaction analysis of the 3% clusters reveals that over the range of sequences generated for each site (9200 to 35500), bacterial diversity increases with increasing number of sequences two to four times faster than archaeal diversity (Fig. S1). Despite the large number of amplicons analyzed, deeper sequencing would be required to fully capture the bacterial diversity of each sample. In contrast, archaeal communities appear to plateau at about 500 OTUs, suggesting that total archaeal diversity is relatively well represented (Fig. S1).

Variation in DCM Community Composition within the SPG

We combined our SPG molecular results with environmental data to test effects of distance and environmental properties on community composition and diversity. Bray-Curtis similarity indices, based on species-level taxon assignments, indicate that, from station to station, there was a strikingly similar bacterial community (>70% similarity) within the SPG. We examined the influence of geography by using non-metric

multidimensional scaling (nMDS), similarity profiles (SIMPROF), and agglomerative hierarchical clustering analysis (Fig. 4 and 5). There is a clear spatial gradient in microbial community composition as western stations 1, 2 and 3, central stations 4-7, and southern stations 9 and 10 define three separate groupings. We performed a SIMPROF test to determine if the samples within each grouping are statistically indistinguishable within a 95% confidence interval (Fig. 5). These groupings correspond to those that result from the nMDS analysis, except that the nMDS analysis further differentiates bacterial communities of the deepest stations 4 and 7 separately from station 5. Archaeal samples also remained true to the nMDS with central Stations 2, 3, 4 and7 clustering together; this likely results from their similar proportions of Marine group II and Marine group III Euryarchaeota (Fig. 2).

Comparison to DCM Community Composition in Other Regions

To test if microbial communities in the DCM of the SPG are distinct from those of other regions, we used bacterial tag populations from the DCM of the NPG and EQP as out-groups. Our analysis of similarity (ANOSIM) analysis ($\rho = 1$, significance = 0.1%) shows that samples from the SPG partition from those of the EQP and NPG despite striking similarities in their proportion and presence of identical dominant pyrotags (Fig. 6). A similarity percentage (SIMPER) analysis, which can be used to identify species that contribute most to the dissimilarity between groups, demonstrated the abundance of SAR 11 to be the discriminating factor between the gyres (30% of dissimilarity) and *Flavobacteriaceae* to be influential in distinguishing the equatorial upwelling sites (15% of dissimilarity).

This distinct SPG bacterial assemblage is broadly similar throughout the central SPG despite the great distances between sites, grouping at >70% similarity at the 3% OTU level. The samples from all three regions (SPG, NPG and EQP) group together at the 50% similarity level, indicating that much of the DCM bacterial community is relatively consistent regardless of region. However, at higher levels of similarity, the SPG, NPG and EQP samples group independently from each other, indicating that these different regions host distinct DCM bacterial communities.

Environmental and Geographic Drivers of Community Structure

To evaluate whether or not environmental variables correlated with community composition of the SPG DCM, we performed a Spearman rank correlation test (RELATE) that compared a matrix of each environmental variable measured with a matrix of calculated Bray-Curtis dissimilarities scores. Bacterial community composition, within the gyre, strongly correlate with sea-surface chlorophyll content (ρ= 0.627, significance= 0.1%)), temperature (ρ= 0.516, significance= 0.3%)), salinity (ρ= 0.407, significance= 3.1%), dissolved nitrate (ρ= 0.368, significance= 3.1%)) and dissolved phosphate (ρ= 0.511, significance= 0.5%)). We also observed several significant environmental variables that corresponded to archaeal community composition including dissolved nitrite (ρ= 0.457, significance= 1.6%) and dissolved nitrate (ρ= 0.374, significance= 2%) (Halm et al. 2011).

To expand upon these results, we complimented these individual correlation tests with a BIOENV analysis that selected a subset of the collected environmental data that would best explain our bacterial and archaeal ordination (Clarke & Gorley 2006). The BIOENV analysis revealed (i) the best predictor of bacterial community composition to

be a combination of sea-surface chlorophyll content and *in situ* temperature ($\rho = 0.763$, significance 1%) and the best predictor of archaeal community composition to be a combination of nutrient availability and temperature ($\rho = 0.492$, significance 8%).

Because sea-surface chlorophyll content is the best individual predictor of bacterial community composition within the DCM of the SPG ($\rho = 0.627$, significance= 0.1%)), we used an environmental fitness analysis (EnvFit) to determine if the relationship persists on an ocean-wide scale. To accomplish this goal, we compared bacterial community composition from the SPG, EQP and NPG sites to annually averaged SeaWiFS sea surface chlorophyll data. The resulting correlation is significant ($r^2 = 0.71$, $p<0.003$).

Recent investigations into the potential for spatial limitations in microorganisms have challenged the once held belief that geography does not constrain the dispersal of microorganisms (Papke et al. 2003, Whitaker et al. 2003, Schauer et al. 2010). In order to examine the influence of geographic distance on community composition regionally (within the SPG) and globally (including the EQP and NPG), we converted latitude and longitude into a pair-wise distance matrix and ran a spearman rank correlation test (permutations=999). Both tests, regional and global, indicate that geographic distance significantly correlates to bacterial community composition in both the SPG ($\rho = 0.529$, significance 0.1%) as well as between all stations analyzed ($\rho = 0.755$, significance 0.1%). Although these correlations to geographic distance are significant, their meaning remains unclear because the most distant sample locations also differ in significant environmental properties.

DISCUSSION

Taxonomic richness in the DCM

Our discovery of high OTU richness for DCM bacterial assemblages in the hyper-oligotrophic SPG supports similar observations of microbial richness in other nutrient-limited marine environments. For example, high taxonomic richness of bacteria occurs at the DCM in both the Sargasso Sea and the NW Mediterranean Sea (Treusch et al. 2009, Pommier et al. 2010). Rarefaction analysis corroborates this claim by showing total bacterial taxa to be under-sampled at every SPG site. In contrast, archaeal richness is much lower than bacterial richness in our SPG samples, as in other previously studied marine environments (Aller & Kemp 2008, Winter et al. 2008).

Within the SPG, bacterial taxonomic richness was lowest at gyre-margin stations 1, 9 and 10 and highest at stations 5 and 6 in the gyre center, where the DCM extends to greater depths than anywhere else on the planet (Fig. S1). This result does not agree with recent observations of decreased richness with increasing latitude (Fuhrman et al. 2008, Sul et al. 2013); instead, bacterial richness in the SPG appears related to mean sea-surface productivity. The geographic variation in richness that we observe in the SPG is unlikely to be an artifact of short-term variation, such as phytoplankton blooms; no satellite evidence of variation in sea-surface productivity occurs at any of our stations in the week prior to the sampling date of each station. We observed no geographic trend in archaeal richness within the gyre.

Treush et al. (2009) reported a shift from lower bacterial diversity in surface water to higher diversity at the DCM. Their study showed that the DCM contains a unique community and its results underscore the importance of examining diversity in the DCM

(Treusch et al. 2009). To our knowledge, the richness we observed at the DCM of the SPG is significantly higher than in previous studies of the DCM in other regions (Treusch et al. 2009, Pommier et al. 2010, Friedline et al. 2012). Some of these differences in diversity can be attributed to methological differences between studies; for example, T-RFLP studies, such as those of Treusch et al. (2009) generally sample only relatively abundant taxa, whereas tag-sequencing studies, such as those of Pommier et al. (2010); Friedline et al. (2012); and this study sample both rare and abundant taxa.

Community composition in the DCM

Despite the remarkable richness of bacterial assemblages, their composition is strikingly homogeneous throughout the SPG. This result implies some advantage for all of the major groups that reside in the DCM of this nutrient-limited region. This advantage may reflect phototrophy and streamlined genome content. A majority of the highly abundant organisms, including Marine Group II Euryarcheota, *Prochlorococcus*, *Pelagibacterubique* (SAR11 clade), SAR 86 and unclassified *Flavobacteriaceae*, carry genes that encode machinery for either photosynthesis or phototrophy (Partensky et al. 1999, Sabehi et al. 2004, Campbell et al. 2008, Riedel et al. 2010). Both *Prochlorococcus* and *Pelagibacter ubique* provide excellent examples of genomic streamlining in order to confer an advantage in an oligotrophic environment (Dufresne et al. 2005, Giovannoni et al. 2005, Eiler et al. 2009). The alphaproteobacterium OSC116, a commonly identified constituent of the DCM (Treusch et al. 2009, Giovannoni & Vergin 2012), was not able to be resolved due to our chosen methodology. Other abundant organisms, such as SAR406 in the Deferribacteres cluster, have been found to be highly correlated with

levels of chlorophyll-*a* and have been speculated to benefit directly from phytoplankton exudates (Gordon & Giovanni 1996).

These dominant bacterial and archaeal taxa are also present at other DCM locations such as the Sargasso Sea, Mediterranean Sea and the Southern California Blight (Treusch et al. 2009, Ghai et al. 2010, Beman et al. 2011). Similar trends in community composition were also observed in the Mediterranean and Sargasso Sea, such as the elevated number of tags associated with SAR11 and the overall dominance of *Alphaproteobacteria* and *Cyanobacteria* at this horizon (Treusch et al. 2009, Pommier et al. 2010). The dissimilarity between the DCM of the NPG and that of the SPG is due primarily to the abundance of SAR11 tags; which contribute to 30% of the Bray-Curtis dissimilarity between regions. The abundance of SAR11 gene copy numbers in the NPG (at Station Aloha) correlates with diatom abundance, primary productivity, dissolved organic carbon (DOC) and *Chl-a* (Eiler et al. 2009). A recent survey of photosynthetic picoeukaryotic composition (0-3µm) in the SPG found no evidence of diatoms at either the DCM or in the surface water (Shi et al. 2009). However, diatoms were found at mesotrophic stations just outside the gyre margin. Although both the SPG and NPG are oligotrophic regions, these observations and the relatively higher concentrations of sea-surface chlorophyll at Station Aloha than in the SPG may explain the relatively higher proportion of SAR11 tags at Station Aloha than in the SPG.

While the abundance of SAR11-associated pyrotags was the major distinguishing factor between gyres, the EQP sites were differentiated by their abundance of *Flavobacteriaceae* tags. This group was responsible for 15% of the Bray-Curtis dissimilarity between regions. This distinction highlights the difference in the

productivity of EQP sites 1 and 8, relative to sites in the North and South Pacific Gyres, as this family is associated with high productivity regimes, such as phytoplankton blooms (Pinhassi et al. 2004).

Archaeal Composition in the SPG

Characteristics of the gyre appear to control the composition of archaeal assemblages in the SPG. The rotation of the gyre shapes environmental variables including DCM depth, by elevating the thermocline and nutricline at the gyre margins and depressing them toward the gyre center (Pennington et al. 2006). Lack of upwelling in the gyre center renders the sea surface nutrient-deprived, reducing sea surface primary production. Results from the MDS analysis appear to reflect this phenomenon as the archaeal communities vary with location, not distance, in the gyre (Fig. 4). Archaeal assemblage composition demonstrates a clear shift in the abundance of MG II and MG III Euryarcheota in transects from the western and southern gyre margin toward the more oligotrophic central gyre stations (Fig. 2). The cause of this shift is unclear; MGIII Euryarcheota are generally considered to be rare (Massana et al. 2000, Galand et al. 2009). Only one other study has identified a MGIII-dominated community; which is in cold deep water in the western Arctic Ocean (Galand et al. 2009). The ecological role of this often rare but ubiquitous archeon is presently enigmatic.

Community Similarity and Habitat Partitioning

In 2006, Hewson and colleagues discovered that composition of bacterial communities is remarkably consistent in oligotrophic surface waters over a horizontal spatial scale of a few kilometers (Hewson et al. 2006). They described this phenomenon as a “Patch Size of Homogeneity”, which they observed to breakdown over 15-50 km

scales. This “Patch Size” was greatly expanded by a study targeting multiple water masses along a North Atlantic transect from 60°N to 5°S, which demonstrated that samples taken thousands of kilometers apart within a single water mass resembled each other more closely in bacterial community composition then they resembled samples vertically separated by hundreds of meters in water depth (Agogue´ et al. 2011).

Our study expands on the results of Agogué et al. (2011) by demonstrating that both bacterial and archaeal tags are remarkably similar within the even larger region of the SPG. Throughout the SPG, the sampled bacterial and archaeal populations differ by only 12.5-28% and 2-16%, respectively, at the 97%-similarity taxonomic level in terms of a Bray-Curtis dissimilarity scores. This similarity is striking, as the sampled locations are horizontally separated by 100s to 1000s of kilometers of open ocean and differ in water depth by up to 100 meters.

Agogué et al. (2011) attributed community differences between water masses to physical barriers to dispersal. However, our results suggest that environmental preferences (illustrated by strong correlations to sea-surface properties such as chlorophyll and temperature) may be more important than barriers to dispersal in defining community composition; bacterial assemblages of the environmentally analogous NPG samples more closely resemble those from our SPG samples than either resembled the assemblages from the nutrient- and chlorophyll-rich samples of the geographically closer EQP.

Despite their similarities, the SPG and NPG communities have distinct taxonomic compositions (> 45% dissimilarity). Differences in the proportion of the dominant taxa as well as differences in the rare community members appear unlikely to result from

differences in sampling season. The SPG gyre samples were taken during the southern hemisphere summer (late December/January 2006/2007) and seasonally corresponded with NPG gyre sample HOT 194 (August 2007). The remaining NPG samples were taken in October (2006) and February (2007) and provide a broad prospective on seasonality within the NPG. As the NPG sample collections occurred at different months and seasons, and these samples are statistically indistinguishable from each other, seasonality alone does not explain differences between the SPG and NPG samples. While relationships between seasonality and DCM communities can be complicated, recent studies have demonstrated highly repeatable seasonal patterns in bacterial community composition in marine surface waters (Fuhrman et al. 2006, Needham et al. 2013). Consequently, differences between the SPG, NPG and EQP in the proportion of dominant community members is likely a direct result of environmental selection. In contrast, differences in presence or absence of rare taxa may reflect allopatric effects, such as currents that block cross-equatorial exchange (e.g., Agogué et al. 2011).

CONCLUSIONS

We sampled DCM prokaryotic communities throughout Earth's largest oceanographic province, the South Pacific Gyre (SPG). This province constitutes 15% of the global ocean area. While differences in community composition along vertical gradients are well documented, few tag-sequencing studies have examined horizontal changes and even fewer have followed an oceanographic horizon, such as the DCM. None have previously examined the SPG. Bacterial and archaeal assemblages are remarkably homogeneous in the DCM of the SPG, as well as across the Pacific. The most abundant taxa are the same at all sites examined, suggesting that these organisms have

adapted to dominate this biologically significant horizon ocean-wide. Significant differences in assemblage composition appear to directly result from environmental heterogeneity. Within the SPG, sea-surface chlorophyll content, *in situ* temperature and *in situ* concentrations of dissolved phosphate and nitrate are all highly correlated to bacterial community composition in the DCM. Of these environmental properties, sea-surface chlorophyll content appears to be the most significant predictor of DCM community structure within the SPG, as well as across the Pacific Ocean, despite large distances between sites and pronounced differences in the depth (up to 200 m), temperature (9.1°C) and other properties of the DCM from one station to another.

Acknowledgements

We thank Captain Tom Desjardins, the crew and the scientific party of *R/V Roger Revelle* Expedition KNOX02RR for the expedition that provided our samples. We thank Rob Pockalny for creating the station location map and Andy Voorhis for trimming the EQP sequencing data. We also thank John Kirkpatrick and Justin Abreu for their reviews of this work. This study was funded by the Ocean Drilling Program and Biological Oceanography Program of the US National Science Foundation (Grants OCE-0527167 and OCE- 0752336).

LITERATURE CITED

Agogue´ H, Lamy D, Neal PR, Sogin ML, Herdnel GJ (2011) Water mass-specificity of bacterial communities in the North Atlantic revealed by massively parallel sequencing. Molecular Ecology 20:258–274

Aller JY, Kemp PF (2008) Are Archaea inherently less diverse than Bacteria in the same environments? FEMS Microbiology Ecology 65:74-87

Baas-Becking LGM (1934) Geobiologie of Inleiding Tot De Milieukund. WP Van Stockum and Zoom (in Dutch): The Hague, the Netherlands

Behrenfeld MJ, Falkowski PG (1997) Photosynthetic rates derived from satelite-based chlorophyll concnetration. Liminology and Oceanography 42:1-20

Beman JM, Steele JA, Fuhrman JA (2011) Co-occurrence patterns for abundant marine archaeal and bacterial lineages in the deep chlorophyll maximum of coastal California. ISME J

Boyle T, Smillie G, Anderson J, Beeson D (1990) A sensitivity analysis of nine diversity and seven similarity indices. Research Journal of the Water Pollution Control Federation 62:749-762

Campbell BJ, Waidner LA, Cottrell MT, Kirchman DL (2008) Abundant proteorhodopsin genes in the North Atlantic Ocean. Environmental Microbiology 10:99-109

Clarke KR, Gorley RN (2006) PRIMER v6: User Manual/Tutorial. In, PRIMER-E, Plymouth

D'Hondt S, Spivack A, Pockalny R, Ferdleman T, Fisher J, Kallmeyer J, Abrams L, Smith D, Graham D, Hasiuk F, Schrum H, Stancin A (2009) Subseafloor sedimentary life in the South Pacific Gyre. Proceedings of the National Academy of Sciences 106:11651-11656

Dufour P, Charpy L, Bonnet S, Garcia N (1999) Phytoplankton nutrient control in the oligotrophic South Pacific subtropical gyre (Tuamotu Archipelago). Marine Ecology Progress Series 179:285-290

Dufresne A, Garczarek L, Partensky F (2005) Accelerated evolution associated with genome reduction in a free-living prokaryote. Genome Biology 6:R14

Eiler A, Hayakawa DH, Church MJ, Karl DM, Rappé MS (2009) Dynamics of the SAR11 bacterioplankton lineage in relation to environmental conditions in the oligotrophic North Pacific subtropical gyre. Environmental Microbiology 11:2291-2300

Fenchel T, Finlay BJ (2004) The ubiquity of small species: patterns of local and global diversity. BioScience 54:777

Friedline CJ, Franklin RB, McCallister SL, Rivera MC (2012) Bacterial assemblages of the eastern Atlantic Ocean reveal both vertical and latitudinal biogeographic signatures. Biogeosciences 9:2177-2193

Fuhrman JA, Hewson I, Schwalbach MS, Steele JA, Brown MV, Naeem S (2006) Annually reoccurring bacterial communities are predictable from ocean conditions. Proceedings of the National Academy of Sciences 103:13104-13109

Fuhrman JA, Steele JA, Hewson I, Schwalbach MS, Brown MV, Green JL, Brown JH (2008) A latitudinal diversity gradient in planktonic marine bacteria. Proceedings of the National Academy of Sciences 105:7774-7778

Galand PE, Casamayor EO, Kirchman DL, Potvin M, Lovejoy C (2009) Unique archaeal assemblages in the Arctic Ocean unveiled by massively parallel tag sequencing. ISME J 3:860-869

Ghai R, Martin-Cuadrado A-B, Molto AG, Heredia IG, Cabrera R, Martin J, Verdu M, Deschamps P, Moreira D, Lopez-Garcia P, Mira A, Rodriguez-Valera F (2010) Metagenome of the Mediterranean deep chlorophyll maximum studied by direct and fosmid library 454 pyrosequencing. ISME J 4:1154-1166

Giovannoni SJ, Tripp H, Givan S, Podar M, Vergin KL, Baptista D, Bibbs L, Eads J, Richardson TH, Noordewier M, Rappe´ MS, Short JM, Carrington JC, Mathur EJ (2005) Genome streamlining in a cosmopolitan oceanic bacterium. Science 309:1242-1245

Giovannoni SJ, Vergin KL (2012) Seasonality in Ocean Microbial Communities. Science 335:671-676

Gordon DA, Giovanni SJ (1996) Detection of stratified microbial populations related to Chlorobium and Fibrobacter Species in the Atlantic and Pacific Oceans. Applied and Environmental Microbiology 62:1171–1177

Gregg WW, Casey NW, McClain CR (2005) Recent trends in global ocean chlorophyll. Geophysical Research Letters 32:L03606

Halm H, Lam P, Ferdelman TG, Lavik G, Dittmar T, LaRoche J, D'Hondt S, Kuypers MMM (2011) Heterotrophic organisms dominate nitrogen fixation in the South Pacific Gyre. ISME J 6:1238-1249

Hewson I, Capone DG, Steele JA, Fuhrman JA (2006) Influence of Amazon and Orinoco offshore surface water plumes on oligotrophic bacterioplankton diversity in the West Tropical Atlantic. Aquatic Microbial Ecology 43:11-22

Huber JA, Mark Welch DB, Morrison HG, Huse SM, Neal PR, Butterfield DA, Sogin ML (2007) Microbial Population Structures in the Deep Marine Biosphere. Science 318:97-100

Huisman J, Pham Thi NN, Karl DM, Sommeijer B (2006) Reduced mixing generates oscillations and chaos in the oceanic deep chlorophyll maximum. Nature 439:322-325

Huse S, Huber J, Morrison H, Sogin M, Welch D (2007) Accuracy and quality of massively parallel DNA pyrosequencing. Genome Biology 8:R143

Huse SM, Dethlefsen L, Huber JA, Welch DM, Relman DA, Sogin ML (2008) Exploring microbial diversity and taxonomy using SSU rRNA hypervariable tag sequencing. PLOS Genetics 4:1-10

Huse SM, Welch DM, Morrison H, Sogin ML (2010) Ironing out the wrinkles in the rare biosphere through improved OTU clustering. Environmental Microbiology 12:1889-1898

Karl DM, Lukas R (1996) The Hawaii Ocean Time-series (HOT) program: Background, rationale and field implementation. Deep-Sea Research II 43:129-156

Martiny JBH, Eisen JA, Penn K, Allison SD, Horner-Devine MC (2011) Drivers of bacterial β-diversity depend on spatial scale. Proceedings of the National Academy of Sciences 108:7850-7854

Massana R, DeLong EF, Pedrós-Alió C (2000) A Few Cosmopolitan Phylotypes Dominate Planktonic Archaeal Assemblages in Widely Different Oceanic Provinces. Applied and Environmental Microbiology 66:1777–1787

Morel A, Gentili B, Claustre H, Babin M, Bricaud A, Ras J, Tieche F (2007) Optical properties of the ''clearest'' natural waters. Liminology and Oceanography 52:217-229

Needham DM, Chow C-ET, Cram JA, Sachdeva R, Parada A, Fuhrman JA (2013) Short-term observations of marine bacterial and viral communities: patterns, connections and resilience. ISME J 7:1274-1785

Oksansen J, Blanchet GF, Kindt R, Legendre P, O'Hara RB, Simpson GL, Solymos P, Henry M, Stevens H, Wagner H (2011) vegan: community ecology package. In: 1.17.12 Rpv (ed)

Papke RT, Ramsing N, B.,, Bateson MM, Ward DM (2003) Geographical isolation in hot spring cyanobacteria. Environmental Microbiology 5:650-659

Partensky F, Hess WR, Vaulot D (1999) Prochlorococcus, a marine photosynthetic prokaryote of global significance. Microbiology and Molecular Biology Reviews 63:106–127

Pennington TJ, Mahoney KL, Kuwahara VS, Kolber DD, Calienes R, Chavez FP (2006) Primary production in the eastern tropical Pacific: A review. Progress in Oceanography 69:285-317
Pinhassi J, Sala MM, Havskum H, Peters F, Guadayol Os, Malits A, Marrase´ Cl, Jansen R (2004) Changes in Bacterioplankton Composition under Different Phytoplankton Regimens. Applied and Environmental Microbiology 70:6753-6766
Polovina J, Howell E, Abecassis M (2008) Ocean's least productive waters are expanding. Geophysical Research Letters 35:5 pp
Pommier T, Neal PR, Gasol JM, Coll M, Acinas SG, Pedrós-Alió C (2010) Spatial patterns of bacterial richness and evenness in the NW Mediterranean Sea explored by pyrosequencing of the 16S rRNA. Aquatic Microbial Ecology 61:221-233
Riedel T, Tomasch J, Buchholz I, Jacobs J, Kollenberg M, Gerdts G, Wichels A, Brinkhoff T, Cypionka H, Wagner-Do¨bler I (2010) Constitutive expression of the proteorhodopsin gene by a Flavobacterium strain representative of the proteorhodopsin-producing microbial community in the North Sea. Applied and Environmental Microbiology 76:3187–3197
Sabehi G, Béjà O, Suzuki MT, Preston CM, DeLong EF (2004) Different SAR86 subgroups harbour divergent proteorhodopsins. Environmental Microbiology 6:903-910
Schauer R, Bienhold C, Ramette A, Harder J (2010) Bacterial diversity and biogeography in deep-sea surface sediments of the South Atlantic Ocean. ISME J 4:159-170
Shi XL, Marie D, Jardillier L, Scanlan DJ, Vaulot D (2009) Groups without Cultured Representatives Dominate Eukaryotic Picophytoplankton in the Oligotrophic South East Pacific Ocean. PLOS One 4
Sogin M, Morrison H, Welch D, Huse S, Neal P, Arrieta J, Herndl G (2006) Microbial diversity in the deep-sea and the unexplored "rare Biosphere". Proceedings of the National Academy of Sciences 103:12115-12120
Sul WJ, Oliver TA, Ducklow HW, Amaral-Zettler LA, Sogin ML (2013) Marine bacteria exhibit a bipolar distribution. Proceedings of the National Academy of Sciences 110:2342-2347
Treusch AH, Vergin KL, Finlay LA, Donatz MG, Burton RM, Carlson CA, Giovannoni SJ (2009) Seasonality and vertical structure of microbial communities in an ocean gyre. ISME J 3:1148-1163
Weston K, Fernand L, Mills DK, Delahunty R, Brown J (2005) Primary production in the deep chlorophyll maximum of the central North Sea. Journal of Plankton Research 27:909-922
Whitaker RJ, Grogan DW, Taylor JW (2003) Geographic Barriers Isolate Endemic Populations of Hyperthermophilic Archaea. Science 301:976-978
Winter C, Moeseneder M, Herndl G, Weinbauer M (2008) Relationship of Geographic Distance, Depth, Temperature, and Viruses with Prokaryotic Communities in the Eastern Tropical Atlantic Ocean. Microbial Ecology 56:383-389

Station #	Station 1	Station 2	Station 3	Station 4	Station 5	Station 7	Station 9	Station 10
Latitude (S)	-23°51,046'S	-26°03,0888'S	-27°56,539'S	-26°28,924'S	-28°26,781'S	-27°44,476'S	-39°18,616'S	-41°51,128'S
Longitude (W)	165°38,637'W	156°53,6494'W	148°35,388'W	137°56,402'W	131°23,423'W	117°37,185'W	139°48,035'W	153°06,284'W
Sampling time (dec.hrs)	20.42	20.73	16.97	19.48	6.32	2.45	21.07	6.42
depth (m)	100	110	120	150	145	200	110	100
Phosphate (µM)	0.00	0.02	0.06	0.07	0.08	0.03	0.93	0.93
Nitrate (µM)	0.08	0.25	0.21	0.25	0.34	0.14	5.39	4.24
Ammonium (µM)	0.04	0.03	0.03	0.03	b/d	0.06	0.17	0.12
Nitrite (µM)	0.07	0.06	0.05	0.04	0.10	0.07	0.46	0.51
sigma theta (kg/m3)	25.76	26.40	26.04	25.97	26.19	26.32	26.67	26.50
salinity (psu)	35.61	35.89	35.51	35.51	35.39	35.49	34.35	34.47
temperature (˚C)	19.64	18.16	18.62	19.39	18.10	18.82	10.80	10.50
Conductivity (S/cm)	4.83	4.68	4.72	n/a	4.65	4.74	3.83	3.81
Chl"*a* (µg/L)	n/a	0.39	0.29	0.21	0.34	0.23	0.36	0.34
Seasurface Chi"*a* (µg/L)	0.05	0.05	0.04	0.03	0.04	0.03	0.11	0.12

Table 1: Environmental characteristics of the samples from the DCM of the South Pacific Gyre.

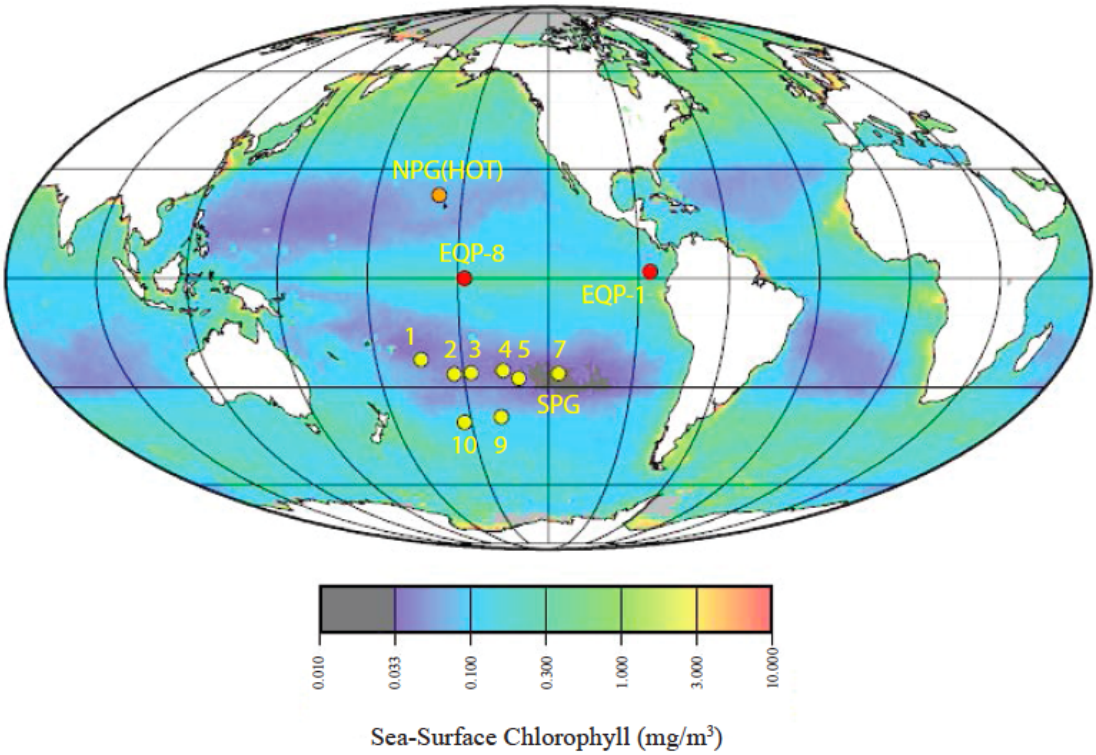

Fig. 1: Locations of sampling stations. Superimposed chlorophyll *a* content was a collected annual average (mean from September 1994-December 2004) from SeaWiFS satellite data that was uploaded into GeoMapApp (Behrenfeld and Falkowski, 1997; Gregg et al., 2005; Ryan et al., 2009). South Pacific Gyre (SPG) sites are indicated by yellow circles. Equatorial Pacific (EQP) and North Pacific Gyre (NPG) stations are represented by orange and red circles, respectively.

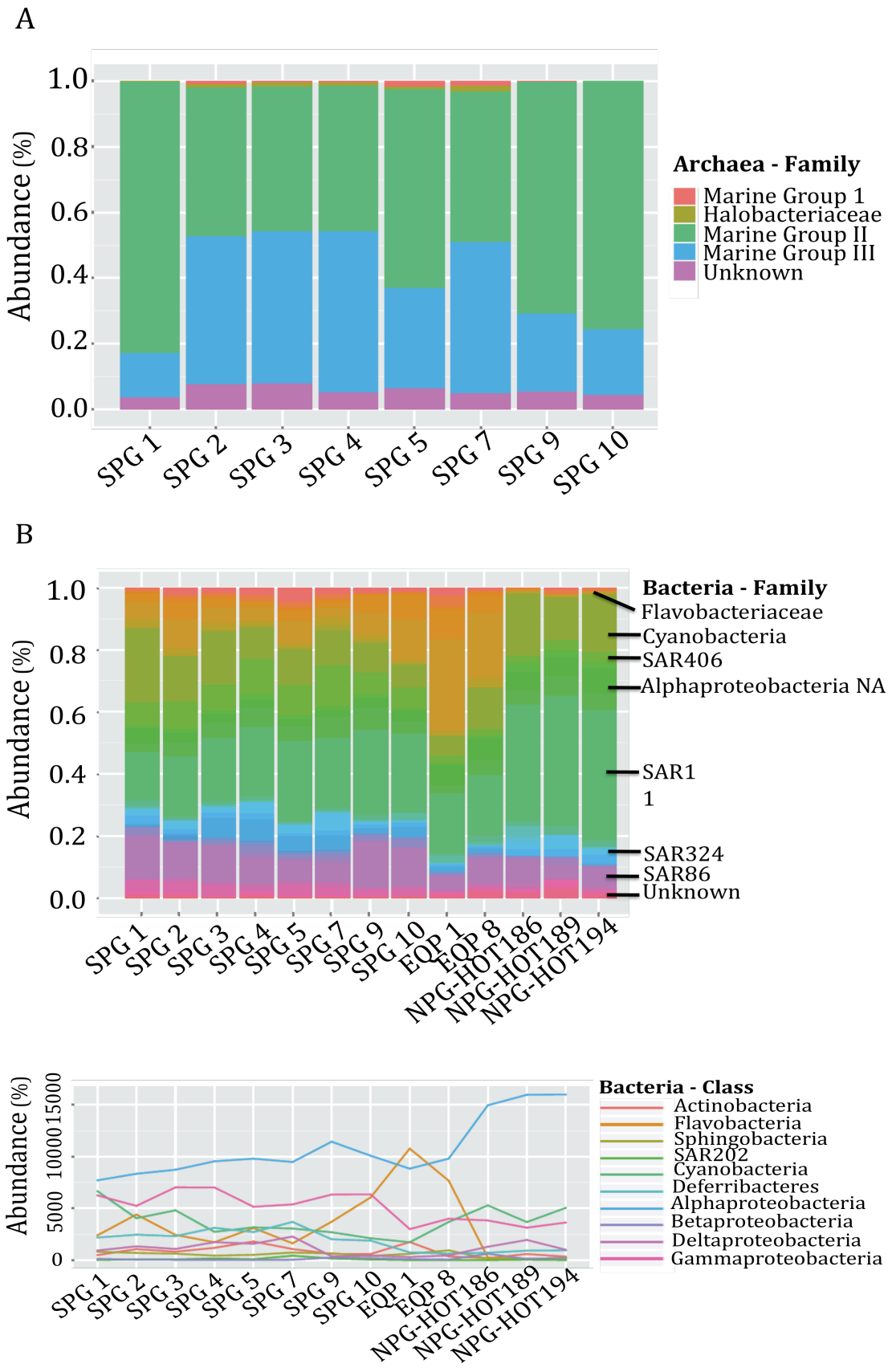
A
Abundance (%)
1.0
0.8
0.6
0.4
0.2
0.0
SPG 1
SPG 2
SPG 3
SPG 4
SPG 5
SPG 7
SPG 9
SPG 10
Archaea - Family
Marine Group 1
Halobacteriaceae
Marine Group II
Marine Group III
Unknown
B
Abundance (%)
1.0
0.8
0.6
0.4
0.2
0.0
SPG 1
SPG 2
SPG 3
SPG 4
SPG 5
SPG 7
SPG 9
SPG 10
EQP 1
EQP 8
NPG-HOT186
NPG-HOT189
NPG-HOT194
Bacteria - Family
Flavobacteriaceae
Cyanobacteria
SAR406
Alphaproteobacteria NA
SAR11
SAR324
SAR86
Unknown
Abundance (%)
0
5000
10000
15000
SPG 1
SPG 2
SPG 3
SPG 4
SPG 5
SPG 7
SPG 9
SPG 10
EQP 1
EQP 8
NPG-HOT186
NPG-HOT189
NPG-HOT194
Bacteria - Class
Actinobacteria
Flavobacteria
Sphingobacteria
SAR202
Cyanobacteria
Deferribacteres
Alphaproteobacteria
Betaproteobacteria
Deltaproteobacteria
Gammaproteobacteria

Fig. 2: (A) Archaeal and (B) Bacterial community composition profiles. Relative abundance of dominant bacterial taxa (Alphaproteobacteria, Gammaproteobacteria, Bacteroidetes and Cyanobacteria) and archaeal taxa (Marine Group II and Marine Group III Euryarcheota) as determined using the GAST (global assignment of sequence taxonomy) system for tag identification.

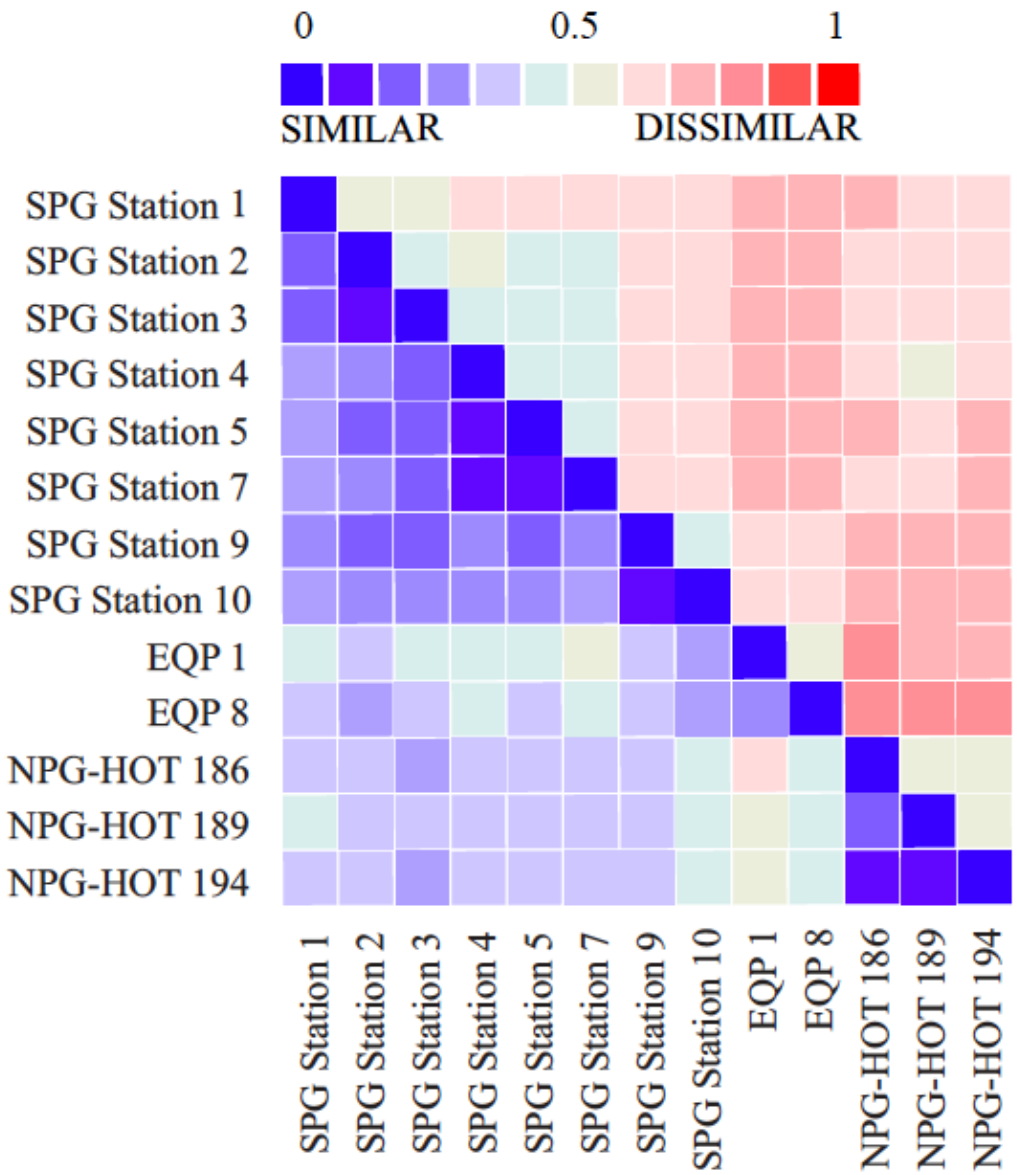

Fig. 3: Bacterial split-heat map featuring the Bray-Curtis (lower left triangle) and Jaccard Index (upper right triangle) as calculated for the pair-wise similarity of species-level taxonomic assignments between the Eastern and Central EQP, NPG and SPG stations where a score of 0(blue) indicates that the communities are identical and a score of 1 (red) indicates that they are completely dissimilar.

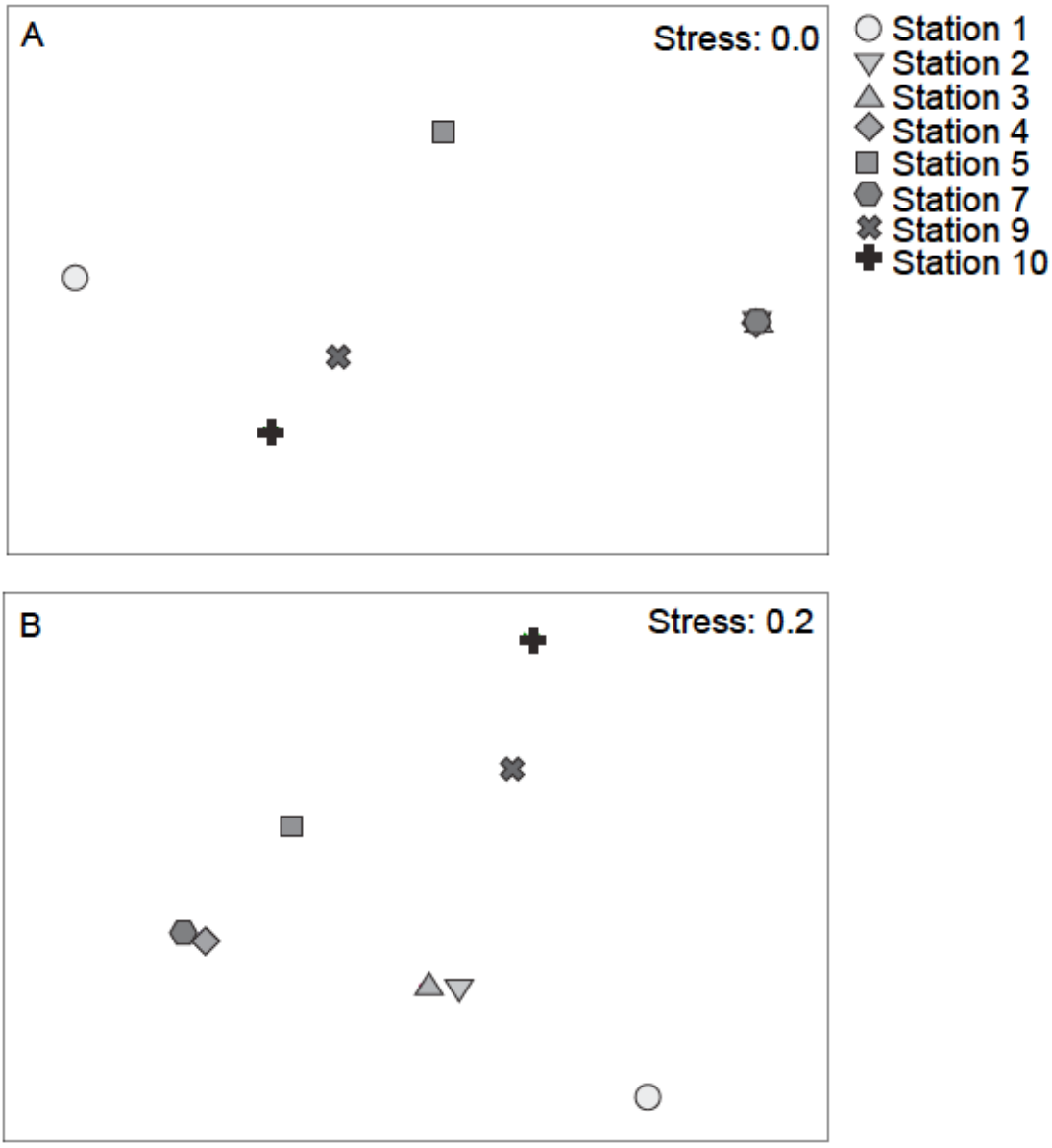

Fig. 4: Non-metric Multidimensional Scaling (nMDS) plots of the SPG stations were generated from archaeal (A) and bacterial (B) species-level taxonomic assignments and subsequent Bray-Curtis dissimilarity matrices (permutations= 999).

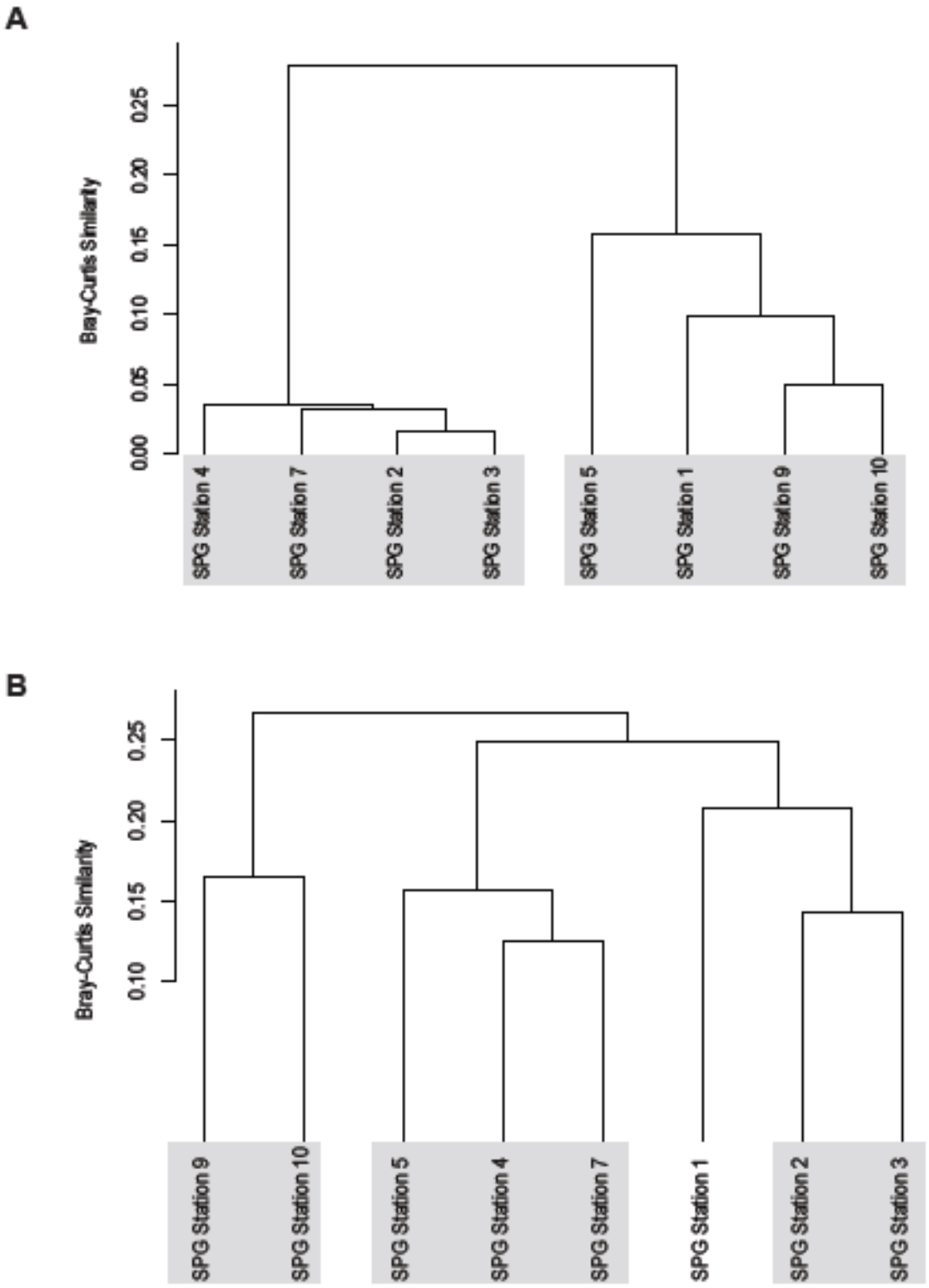
A
Bray-Curtis Similarity
0.00
0.05
0.10
0.15
0.20
0.25
SPG Station 4
SPG Station 7
SPG Station 2
SPG Station 3
SPG Station 5
SPG Station 1
SPG Station 9
SPG Station 10
B
Bray-Curtis Similarity
0.10
0.15
0.20
0.25
SPG Station 9
SPG Station 10
SPG Station 5
SPG Station 4
SPG Station 7
SPG Station 1
SPG Station 2
SPG Station 3

Fig. 5: Dendrograms were generated from an agglomerative "group average" cluster analysis of archaeal (A) and bacterial (B) community Bray-Curtis similarity (0 = 100% similar), based upon species-level taxonomic assignments, at the DCM between each station. Statistically identical samples, $p<0.05$, were identified by a SIMPROF test and are highlighted by the grey boxes.

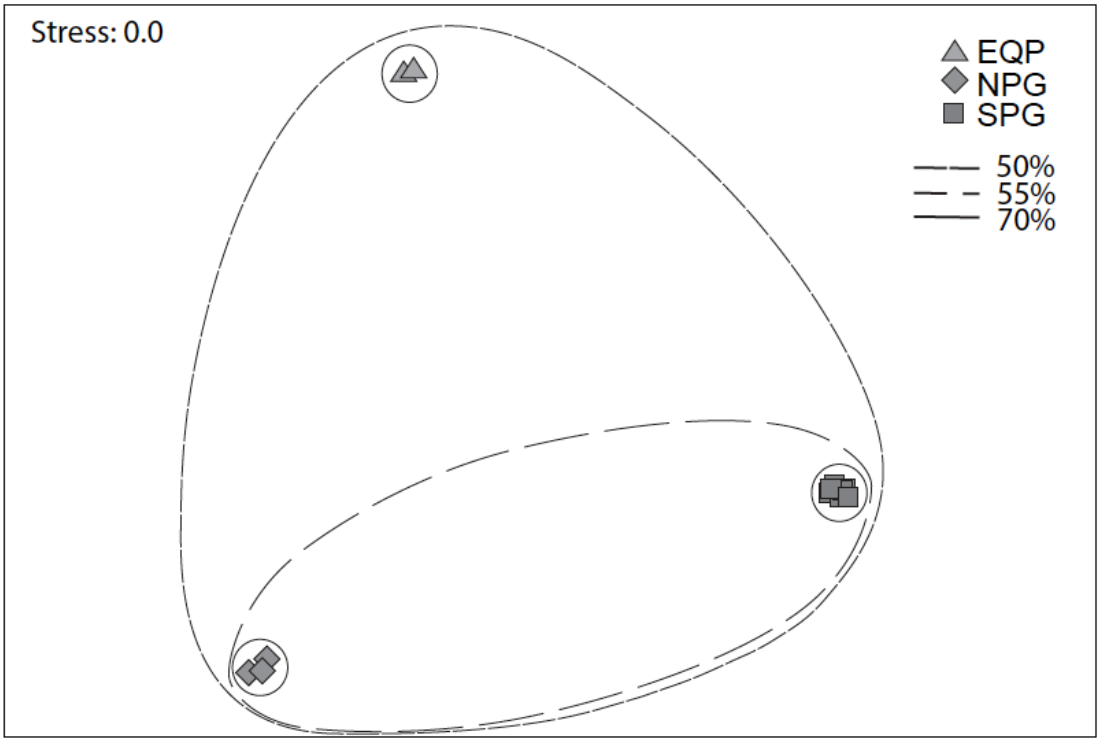

Fig. 6: Non-metric Multidimensional Scaling (stress: 0.0) was performed on species-level taxonomic assignments and the corresponding data matrix subjected to an ANOSIM (analysis of similarity, permutations = 999, distance = "bray"). Samples taken from each environment clustered accordingly and remained distinct from each other with a p-value= 0.001 and R=1. Dashed and solid lines denote Bray-Curtis sample similarity for the South Pacific Gyre (■, SPG), Equatorial Pacific (▲, EQP) and North Pacific Gyre (♦, HOT).

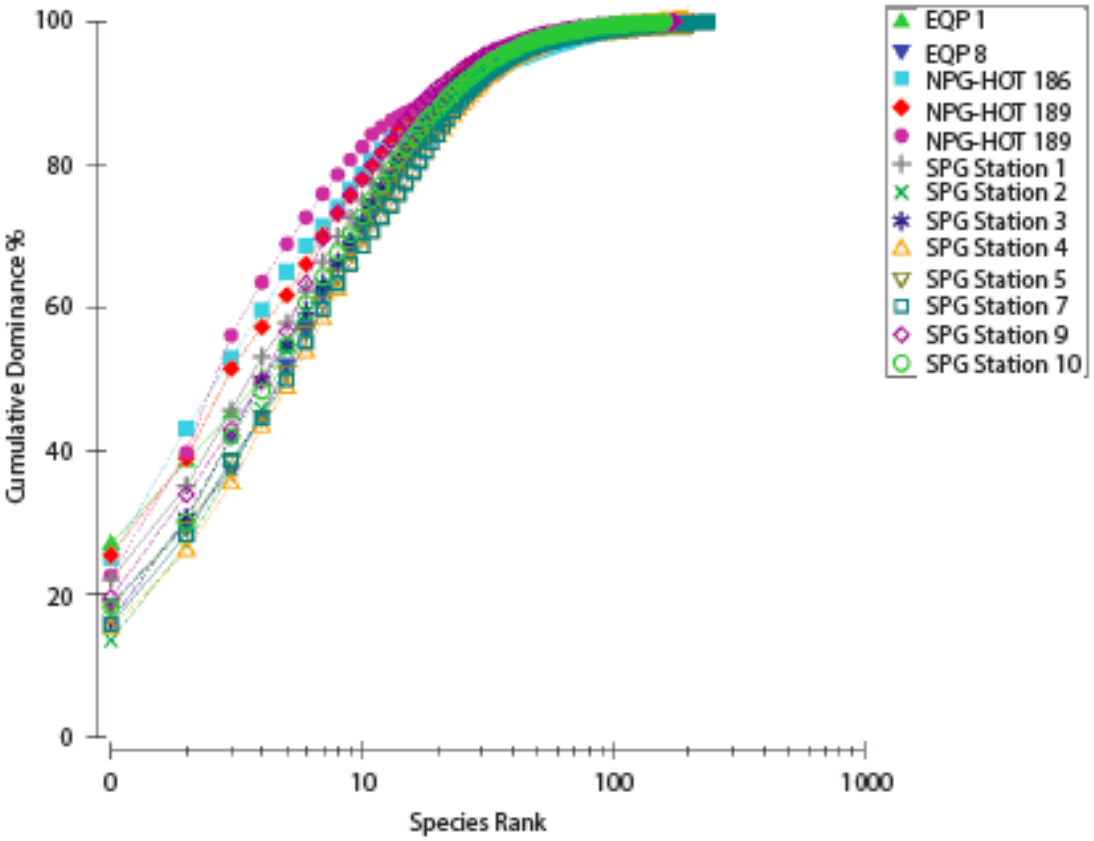
Cumulative Dominance %
100
80
60
40
20
0
0
10
100
1000
Species Rank
EQP 1
EQP 8
NPG-HOT 186
NPG-HOT 189
NPG-HOT 189
SPG Station 1
SPG Station 2
SPG Station 3
SPG Station 4
SPG Station 5
SPG Station 7
SPG Station 9
SPG Station 10

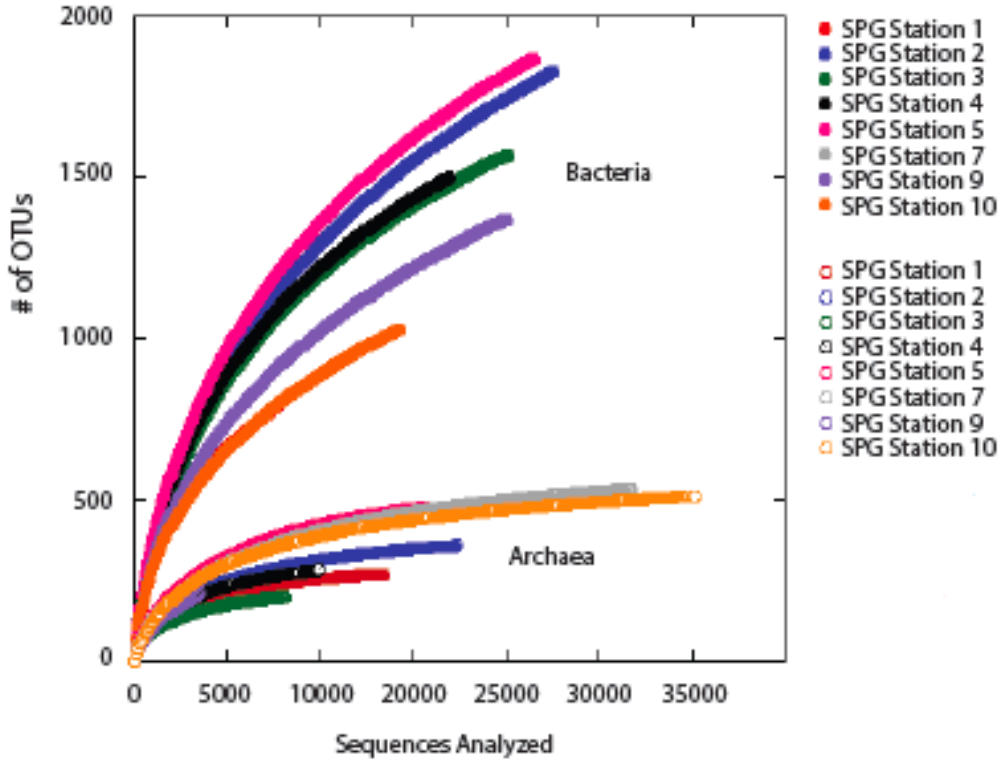
# of OTUs
2000
1500
1000
500
0
0
5000
10000
20000
25000
30000
35000
Sequences Analyzed
Bacteria
Archaea
SPG Station 1
SPG Station 2
SPG Station 3
SPG Station 4
SPG Station 5
SPG Station 7
SPG Station 9
SPG Station 10
SPG Station 1
SPG Station 2
SPG Station 3
SPG Station 4
SPG Station 5
SPG Station 7
SPG Station 9
SPG Station 10

Fig. S1: (A) Species abundance plot demonstrating the cumulative percent dominance of observed species-level taxonomic assignments in order of their rank abundance for SPG, EQP and NPG stations. (B) OTU richness was examined through rarefaction analysis of both bacterial and archaeal communities. Sequences for both bacteria (●) and archaea (○) were clustered at the 3% similarity for each station.

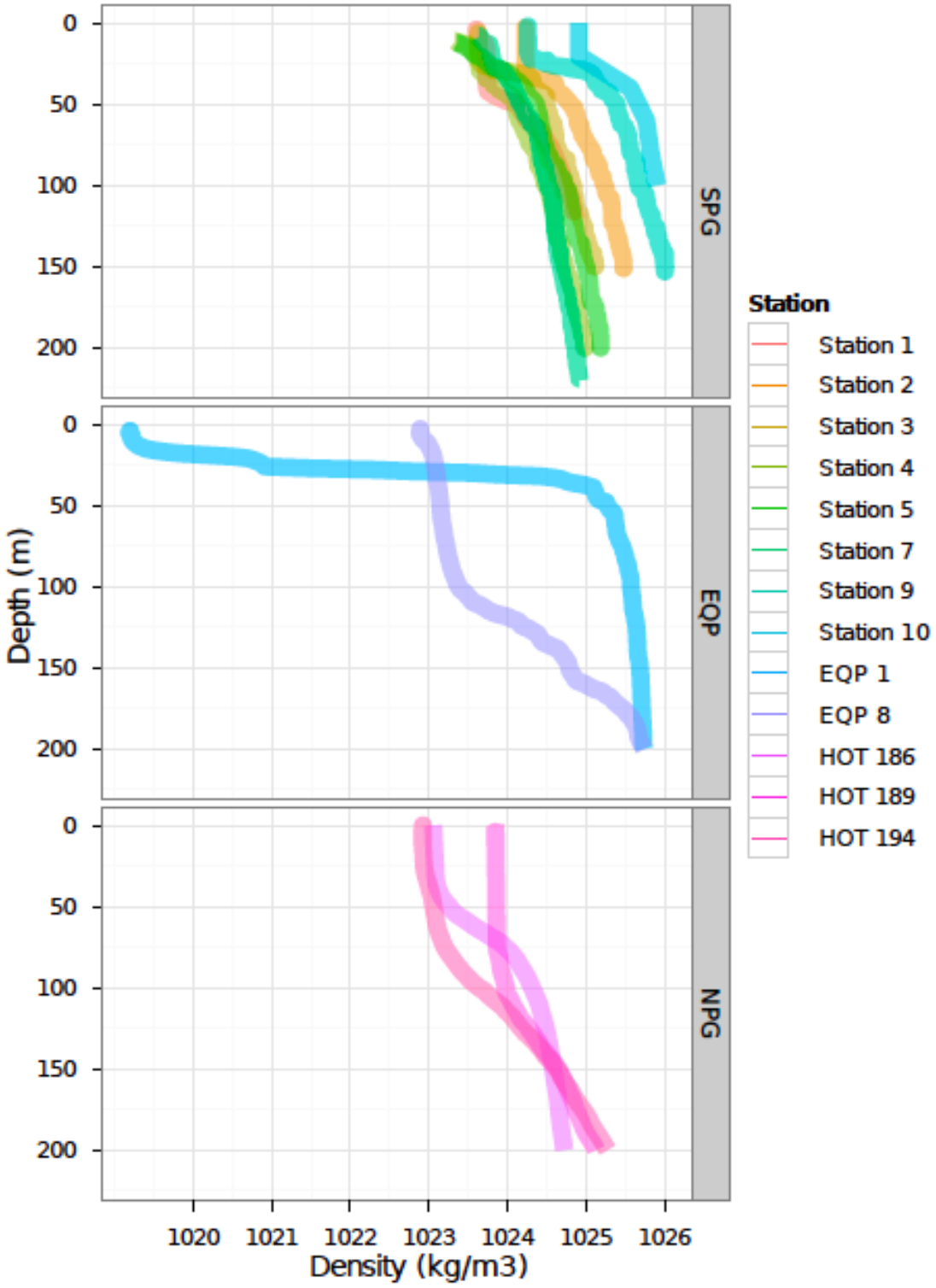

Fig. S2: Density profiles for the SPG, NPG and EQP Stations.

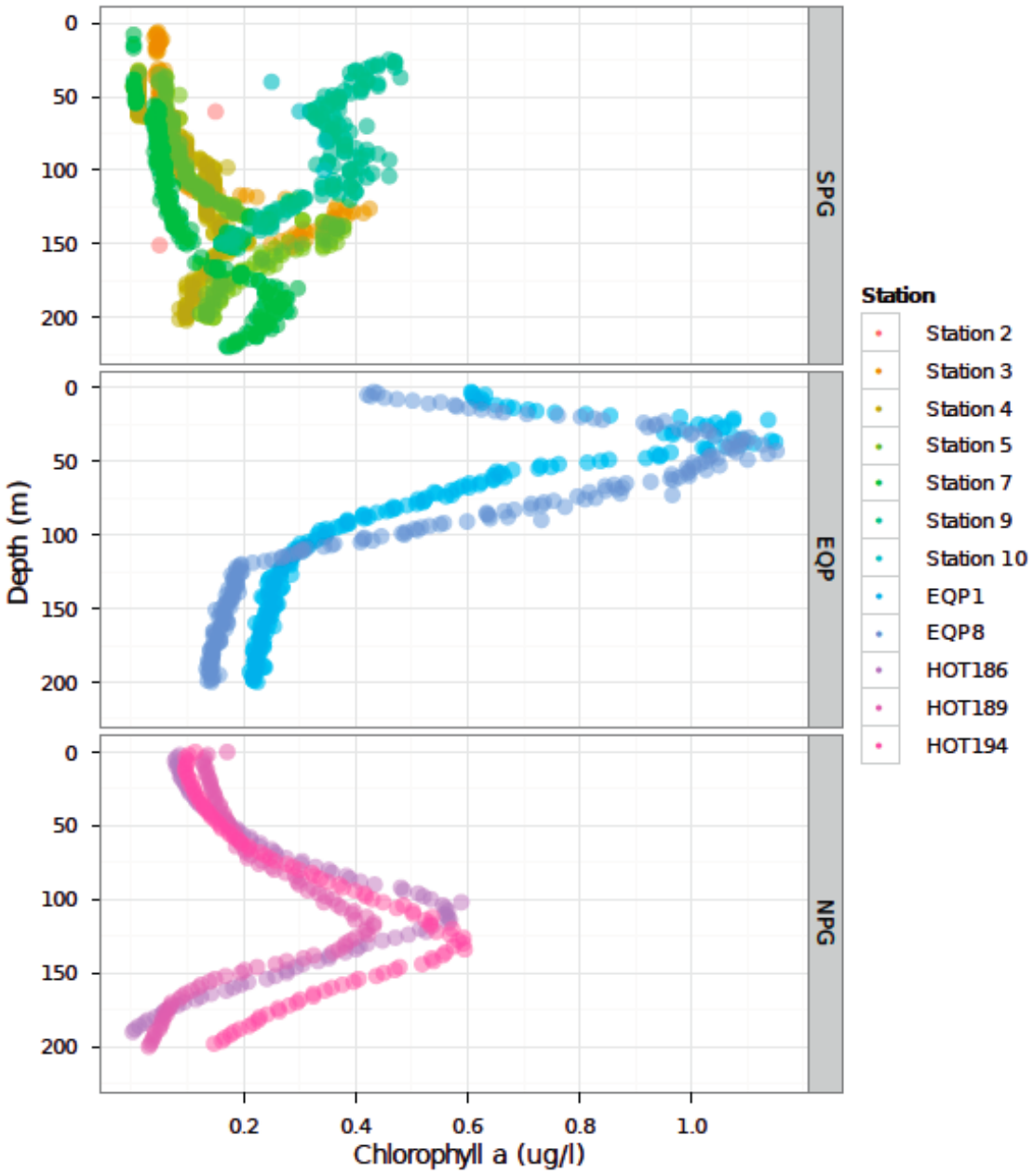

Fig. S3: Chlorophyll profiles for the SPG, NPG and EQP Stations.

MANUSCRIPT II

VERTICAL CHANGES IN BACTERIAL DIVERSITY AND COMMUNITY COMPOSITION FROM SEASURFACE TO SUBSEAFLOOR

By

Emily A. Walsh[1], John B. Kirkpatrick[1], Robert Pockalny[1], David C. Smith[1], Mitchell Sogin[2], Steven D'Hondt[1]

[1] Graduate School of Oceanography, University of Rhode Island, Narragansett Bay Campus, 215 South Ferry Road, Narragansett, RI 02882, USA

[2]Josephine Bay Paul Center for Comparative Molecular Biology and Evolution, Marine Biological Laboratory, 7 MBL Street, Woods Hole, MA 02543, USA

To be submitted to ISME J Fall 2014

Vertical changes in bacterial diversity and community composition from seasurface to subseafloor

Emily A. Walsh[1], John B. Kirkpatrick[1], Robert Pockalny[1], David C. Smith[1], Mitchell Sogin[2], Steven D'Hondt[1]

[1] Graduate School of Oceanography, University of Rhode Island, Narragansett Bay Campus, 215 South Ferry Road, Narragansett, RI 02882, USA
[2]Josephine Bay Paul Center for Comparative Molecular Biology and Evolution, Marine Biological Laboratory, 7 MBL Street, Woods Hole, MA 02543, USA

Classification: Environmental Science

Corresponding author: Emily Walsh, University of Rhode Island, Graduate School of Oceanography, Horn Building 100 B, Narragansett RI 02882.
Fax: (401)-874-6811
Email: ewalsh@gso.uri.edu
Phone: (401) - 874 – 6599

Abstract

We investigated compositional relationships between bacterial communities in the water column and those in deep-sea sediment at three environmentally distinct sites in the Pacific Ocean (two in the Equatorial Pacific and one in the North Pacific Gyre). Through massively parallel pyrosequencing of the v4-v6 hyper-variable regions of the 16S rRNA gene, we characterized 450,104 pyrotags representing 29,814 operational taxonomic units (OTUs) (97% similarity). Hierarchical clustering and non-metric multidimensional scaling partition the samples into four distinct groups, regardless of geographic location: a photic-zone community, a sub-photic community, a shallow sedimentary community, and a deep sedimentary community. Taxonomic richness is highest in the water column and lowest in the deep sediment (≥ 2 meters below seafloor [mbsf]). Within the water column, taxonomic richness is highest in the O_2 minimum zone. In the sediment, taxonomic richness is highest near the seafloor. The most common taxa in the deep sediment are generally present but rare (<0.025%) in the water column and moderately abundant in the shallow sediment (0.05 cm). These results are consistent with (i) dispersal of marine sedimentary bacteria via the ocean, and (ii) selection of the subseafloor sedimentary community from within the community present in the shallow sediment.

Introduction

Broadly similar microbial communities inhabit similar subseafloor sedimentary environments separated by thousands of km (Inagaki et al 2006). This observation is consistent with the old adage, "Everything is everywhere but the environment selects"(Baas-Becking 1934), in which microorganisms are considered to be ubiquitously dispersed due to their small size, large numbers, and low extinction rates (Martiny et al 2006). Distributions of abundant bacterial taxa in surface marine sediment (1 mbsf) suggest that the seafloor is colonized *via* the overlying water

column (Hamdan et al 2013). However, the relationship of microbial communities in deep subseafloor sediment (≥ 2 mbsf) to those in surface marine sediment and the overlying ocean has not been previously examined.

To test the extent to which bacterial communities of deep subseafloor sediment may originate in the water column, we used 454 pyrosequencing technology and the v4-v6 hypervariable region of the bacterial 16S rRNA gene to examine bacterial community composition (presence/absence and relative abundance) in the water column, near-seafloor sediment (5 cm), and subseafloor (≥ 2 meters below seafloor) sediment at three environmentally distinct sites in the Pacific Ocean. We investigated (i) the vertical succession of marine bacterial communities from the seasurface to deep subseafloor sediment, and (ii) how those communities vary from one oceanographic region to another.

Materials and Methods

Sampling Sites and Methodology

We collected sediment and seawater samples during a two-month transect of the *R/V Knorr* through the eastern equatorial Pacific and the North Pacific gyre (*Knorr* Expedition 195-3, January-February 2009). For this study, we analyzed sediment and water samples from three stations that are located in three environmentally distinct regions of the Pacific Ocean: the eastern equatorial upwelling region (EQP1), the open-ocean central equatorial upwelling region (EQP8) and the low-productivity northern gyre (EQP11) (Figure 1).

Sampling the water column and different sediment horizons in distinct regions provides a means to evaluate the influence of local oceanographic properties such as nutrient availability, sedimentation rate and distance from land (Fuhrman et al 2006, Kallmeyer et al 2012) on general depth diversity patterns. In high-productivity regimes, such as the eastern equatorial Pacific upwelling region (EQP 1) and the central equatorial Pacific upwelling region (EQP 8), a relatively high flux of organic debris to the seafloor sustains an active anaerobic subseafloor sedimentary community (D'Hondt et al 2004). High productivity in surface waters can also lead to the formation of oxygen deficient zones in deeper water, such as at EQP 1, where unique communities may form in response to the deoxygenation (Beman and Carolan 2013). In contrast, low-productivity regions, such as the North Pacific gyre (EQP 11), are characterized by an oxic water column, extremely low rates of sedimentation and organic matter deposition, and a relatively low-activity aerobic subseafloor community (D'Hondt et al 2009, Røy et al 2012).

We collected the water samples using a 24- Niskin bottle CTD rosette (Sea-Bird SBE-911 CTD system plus package), of which 5L was drained through a sterile 0.2µm Sterivex™ filter (Millipore) and stored at -80º C. We targeted a combination of standard depths and oceanographic horizons (O_2 minimum, chlorophyll maximum, *etc*.) and analyzed 7 to 14 sampling depths at each station from 3 to 5500 m water depth depending on location. Water depths were measured using the center depth of the SeaBeam 2112 multibeam. By dividing the crustal age (Müller et al 2008) by the sediment thickness, based on the NDGC global thickness grid (Divins 2003), we estimated average rates of sedimentation for each site. Mean annual average

chlorophyll a data (Behrenfeld and Falkowski 1997, Gregg et al 2005), collected from September 1994-December 2004, was utilized as a proxy for sea surface productivity.

At each station, we collected sediment using a multi-corer (0 to 30 cm below seafloor [cmbsf]), gravity corer (up to four meters below seafloor [mbsf]) and long-piston coring device (up to 35 mbsf). We subsampled the sediment using sterile 60 cc cut-off syringes and immediately froze the subsamples at -80º C for later DNA extraction. For each site in this study, we analyzed one sediment sample taken with the multi-corer at the sediment-water interface (0-10 centimeters below seafloor [cmbsf]) and 2 to 5 sediment samples taken at greater depths (between 0.25 and 34 mbsf). In total, this study includes 39 tag-pyrosequencing samples: 28 from the water column, three from the sediment-water interface and eight from deep subseafloor sediment.

Site descriptions

EQP-1 (1° 48.21' N, 86° 11.29' W) represented the easternmost site in our equatorial Pacific transect and the site closest to shore and had a water depth of 2885 meters (Fig 1). This nutrient-rich upwelling region contained a highly productive ecosystem and is characterized by a high sedimentation rate (~72 m/million years, Ma). This site had a pronounced O_2 minimum zone, which we targeted specifically for tag pyrosequencing (along with other significant oceanographic features including sea-surface, O_2 maxima [and secondary minima], chlorophyll-a maximum, thermocline, and deep water). The chlorophyll maximum was strongly developed at this site (34 m depth) and was located above the depth of the pycnocline. The O_2 minimum zone, which resided within the thermocline, contained O_2 concentrations as low as 6

μmol/kg (Figure 2). In the sediment, dissolved oxygen was limited to the upper 7 mm (Røy et al 2012).

EQP-8 (0° 0.36' N, 147° 47.50' W) corresponds to the westernmost site of our equatorial transect (Fig 1). The sedimentation rate at this site (4.8 m/Ma) was substantially lower than at EQP-1. This site was located in the equatorial upwelling region far from the influences of coastal run-off. Consequently, it had high surface productivity for a location so far from shore at a water depth of 4336 m. Oceanographic features that we specifically targeted for tag pyrosequencing included the sea surface, chlorophyll-a maximum, O_2 minimum and deep water. At this site, the chlorophyll maximum formed slightly deeper in the water column at 41 m but, in contrast to EQP1, was above the depth of the pycnocline. The O_2 minimum at this site was within the thermocline, with a concentration of 29 μmol/kg (Figure 2). In the sediment, dissolved oxygen penetrated ~10 cm below seafloor (Røy et al 2012).

EQP-11 (30° 21.32' N, 157° 52.23' W) located in the North Pacific gyre represents our deepest sample at a depth of 5819 m.. Oceanographic features that we targeted specifically for pyrosequencing include the sea surface, salinity transitions, O_2 minimum, and deep water. The deep chlorophyll maximum was not strongly developed and formed at 127 m. The O_2 minimum at this site (18 μmol/kg) was deep in the water column (900 m). As at the other sites, this O_2 minimum was located within the thermocline. The sedimentation rate was extremely low (~1.0 m/Ma). Dissolved oxygen penetrated past the greatest depth cored (28.06 mbsf, (Røy et al 2012).

DNA Extraction, Pyrosequencing and Statistical Analyses

We applied a high-resolution v4-v6 tag pyrosequencing approach of the bacterial 16S rRNA gene to 39 water and sediment samples taken vertically from sea surface to sub-seafloor at three environmentally distinct regions of the Pacific Ocean (Figure 1). We extracted DNA from filtered water samples using the Power Water® DNA Isolation Kit (MoBio, Carlsbad, CA, USA) and from sediment samples using the Power Soil® DNA Isolation Kit (MoBio, Carlsbad, CA, USA). We modified the extraction protocol for the deep EQP-11 sediment samples (2m and 4 m) to overcome effects of low biomass and DNA-binding clay (Cai et al 2006, Kallmeyer et al 2012). These modifications were (i) pooling of 10x the sediment (10 g vs 1 g) and (ii) use of extended PCR cycle numbers (40x vs 30x). Additionally, we used a phenol/chloroform DNA extraction for water column samples from EQP-1. We used fusion primers 518f and 1064r, targeting the v4-v6 hypervariable regions of the 16S rRNA gene, to construct amplicon libraries using the following PCR conditions: 94ºC for 2 minute, 30 cycles of (94ºC for 30 sec, 55ºC for 20sec, 72ºC for 1 min). We pooled three separate PCR reactions per sample to eliminate the potential for early cycle PCR-induced error. We then sequenced these pooled libraries using a FLX 454 pyrosequencer.

We discarded low-quality reads, defined as (i) reads with undefined residues and (ii) reads that did not contain the PCR primers at the beginning of each read (Huse et al 2008). We taxonomically assigned reads, based on ≥ 80 % sequence similarity, using the GAST system for sequence identification (Sogin et al 2006). We used the Qiime program to calculate taxonomic richness (total operational taxonomic units

[OTUs], Chao-1, ACE and Phylogenetic Diversity [PD], (Caporaso et al 2010). To ensure inter-sample comparability for our taxonomic richness estimates, we also utilized the Qiime software to randomly reduce the number of reads in each sample to the lowest number of reads in any individual sample. We used the Primer-E software package (Clarke and Gorley 2006) to calculate Bray-Curtis similarity indices and use them for all ordination and statistical methods including nMDS, hierarchical group-average clustering and Spearman rank correlation tests.

Results

Similarity Among Bacterial Communities

Hierarchical "group-average" clustering and nMDS analyses separate our samples into four distinct abundance-weighted communities, based on Bray-Curtis similarity (Figure 3a). Regardless of site, water-column samples partitioned into photic-zone communities, which included samples from at or above the deep chlorophyll maximum (DCM), and aphotic communities (below the DCM). The GAST taxonomy demonstrated that Cyanobacteria, Flavobacteria and Alphaproteobacteria dominated the photic zone community, while the aphotic zone community was heavily dominated by Alphaproteobacteria, Gammaproteobacteria, Deltaproteobacteria and Deferribacteres (Figure 4). The photic zone samples clearly clustered by site while the aphotic zone samples varied less from site to site. Water column samples declined in similarity with increasing water depth regardless of site location (Figure 3b). Spearman rank correlation tests validated the nMDS results, as

chlorophyll a and depth both varied significantly with bacterial community composition (Figure 3b). We also observed two distinct groups in the sedimentary environment, a shallow (0-10 cmbsf) and a deep (0.25-34 mbsf) sedimentary community. The common members of the shallow sedimentary community overlapped with those of the deep-water community; the shallow sedimentary community was dominated by Alphaproteobacteria, Gammaproteobacteria, Deltaproteobacteria as well as Nitrospira and Planctomycetes (Figure 4). The deep sedimentary community was primarily comprised of members of the obsidian pool (OP) candidate phylum, including OP9, OP8, and OP3, as well as Chloroflexi (Dehalococcoidetes and Anaerolineae), Actinobacteria and other phyla of an unknown lineage (Figure 4).

The Rank Abundance and Distribution of Shared OTUs

To examine the extent to which OTUs were shared between the previously described communities (photic, aphotic, shallow sediment and deep sediment) (Figure 3a), we generated rank abundance histograms of the 100 most abundant OTUs (97% similarity) in each community. We highlighted the OTUs shared between the shallow sedimentary community and the deep sedimentary community (only including samples ≥ 2 mbsf) and between the deep sedimentary community and the water-column communities (photic and aphotic) (Figure 5 a-c). Our clustering results binned an EQP1 sample from 0.25 cmbsf with the deep sedimentary community; however, we have excluded this sample from this analysis because it was taken close to the seafloor

and we wish to ensure that only OTUs truly selected for subseafloor conditions are compared.

Many of the most abundant OTUs in our deep sedimentary community were present in the water at trace levels (<0.025%) (Figure 5c). These shared OTUs belong to Dehalococcoidetes, OP9, OP8, and other taxa. Furthermore, most of the most abundant OTUs in the shallow sediment were present in the deep-sediment community (Figure 5b). In contrast, most of the dominant OTUs from the photic and aphotic water-column communities did not occur in the tags from our deep sedimentary samples. The abundant water-column OTUs that did appear in our deep sedimentary tags included members of the Actinobacteria, Planctomycetes, and Firmicutes (Figure 4). In short, the individual OTUs that were most abundant in the deep sediment were generally moderately abundant in the shallow sediment and generally present but very rare (<0.025% of the tag population) in the overlying water column (Figure 6).

Taxonomic Richness, Evenness and Phylogenetic Diversity

Vertical trends in bacterial diversity (# of observed OTUs, Chao-1, ACE and PD) and evenness (H') were similar at all three sites, with all measurements of richness and evenness peaking within the mesopelagic zone (Table 1). Overall, diversity was highest in the water column and lowest in the deep subseafloor sediment (Figure 2 a). Within the water column, the vertical profile of bacterial diversity mirrored the O_2 profile and matched the profile of apparent oxygen utilization (AOU) at each site (Figure 2 a,b, Table 1). Diversity in the water column was generally lowest in the surface ocean and highest at the O_2 minima (Figure 2 a,b). In the sediment, richness

was highest near the seafloor (Figure 2 a). Bacterial diversity in the water column varied from site to site; for example, richness was highest in the oxygen minimum zone (OMZ) of North Pacific gyre site EQP-11 and much lower in the OMZ of eastern equatorial upwelling Site EQP-1 (Figure 2 a).

Discussion

Vertical Trends in Bacterial Diversity

Water column bacterial communities exhibited a clear depth profile, with samples declining in similarity from the sea-surface to the abyssopelagic waters, in accordance with previously described trends (Brown et al 2009, DeLong et al 2006, Giovannoni et al 1996, Gordon and Giovannoni 1996, Treusch et al 2009, Wright et al 1997). While changes in community composition with depth have previously been well documented, studies of taxonomic richness with depth have yielded mixed results. Some studies have reported declines in taxonomic richness and/or PD with increasing ocean depth (Agogué et al 2011, Brown et al 2009, Bryant et al 2012) while others have observed higher richness deeper in the water column (Ghiglione et al 2012, Jing et al 2013, Kembel et al 2011, Pommier et al 2010, Quince et al 2008, Treusch et al 2009). By sampling the water column more comprehensively than previous studies, we find that bacterial richness (taxonomic richness, PD, Chao-1 and ACE) and evenness in the water column was lowest at the surface and highest within the O_2 minima of the mesopelagic zone at each site. These results were consistent from site to site regardless of the diversity metric applied. Consequently, they provide clear evidence of vertical changes in bacterial richness across a range of environments.

Some previous studies also reported elevated bacterial richness within the mesopelagic zone (Jing et al 2013, Kembel et al 2011, Ladau et al 2013), but did not explicitly associate this result with the O_2 minimum zone. The relationship we observed between oxygen and taxonomic richness suggests that respiration may play a significant role in shaping bacterial richness in the open-ocean.

Only a few studies have examined bacterial diversity in both the water column and marine sediment (Feng et al 2009, Hamdan et al 2013, Zinger et al 2011). None of these studies included sediment deeper than one meter below seafloor. Most previous studies of seafloor bacterial communities agree that those communities are highly diverse (Hewson et al 2007, Luna et al 2004, Madrid et al 2001, Ravenschlag et al 1999, Schauer et al 2010). Some studies have suggested that seafloor communities are taxonomically richer than communities in the water column (Feng et al 2009, Lozupone and Knight 2007, Zinger et al 2011). In our study, taxonomic richness was generally higher in the water and generally lower in the sediment. This difference from previous studies may be partly due to the absence of subseafloor (> 1 mbsf) sedimentary communities in those studies (>1 mbsf communities at our sites tend to be consistently less diverse than seafloor communities). It may also be due to the different oceanographic context of our studies relative to some previous studies (e.g., Feng et al. 2009). It is possible that the open-ocean seafloor sediment is less taxonomically rich than seafloor sediment of continental margins and estuaries. This difference may also partly result from different sampling approaches. Our study and Feng et al (2009) sample both seawater communities and sediment communities at each location, while Luzopone and Knight (2007) and Zinger et al. (2011) compared

seawater communities from diverse locations with sediment communities from very different locations.

Within the sediment at all of our sites, taxonomic richness was highest at the seafloor and declined with increasing sediment depth. We also observed extensive taxonomic overlap between the communities of the deep sediment and those of the shallow sediment. These observations suggest that communities in deep marine sediment are derived from a subset of the community that lived in the sediment when it was near the seafloor.

Water Column and Sediment Harbor Distinct Communities

Zinger and colleagues (2011) examined the bacterial beta-diversity of seafloor and seawater ecosystems and demonstrated that pelagic communities and epibenthic communities differed greatly at all taxonomic levels. Our study supports this observation and extends it to subseafloor sediment, as the abundance-weighted bacterial communities of the sediment are clearly distinct from those in the overlying water column (Figure X).

Taxonomic overlap between the ocean and sediment

When we considered the presence/absence of individual taxa, we observed overlap between environments. The most prominent example of this overlap was the presence in seawater and shallow sediment of the individual OTUs that were most abundant in the deep sediment (Figure 6). This result is consistent with microbes being carried through the water column and deposited in the sediment. The absence of

known phototrophs (e.g., *Prochlorococcus*, *Synechococcus* and SAR11) in our subseafloor tag populations indicates that taxonomic overlap between the water column and subseafloor sedimentary communities does not simply result from preservation of fossil remains. Instead, the subseafloor conditions appear to select for preferential survival of taxa that were represented by relatively few sequences from the water column. This result was not surprising, as subseafloor sedimentary conditions are very different from water-column conditions; for example, anoxic conditions and low energy availability are much more ubiquitous in subseafloor sediment than in the overlying ocean (Jørgensen and D'Hondt 2006). It is therefore possible that microbes associated with the sedimentary environment are re-suspended and transported long distances through the water column where they may or may not re-colonize the seafloor. This result agrees with Hamdan et al.'s (2013) identification of Alaskan Beaufort Shelf sediment as a sink for transiting deep-water OTUs. "Misplaced microbes" are also known to accumulate on the seafloor, as shown by the highly diverse anaerobic thermophilic spore population discovered in the cold arctic sediment of the Svalbard Fjord and the Peru Margin (Hubert et al 2009, Lee et al 2005).

Microbial transport through the water column may explain the incidence of large-scale biogeographic patterns in both near-seafloor sediment (Hamdan et al., 2006) and subseafloor sediment. A previous study (Inagaki et al 2006) observed that similar taxa (class/family level-90% similarity, e.g. Dehalococcoidetes, OP9 and Desulfobacteriales) are present in environmentally similar subseafloor sedimentary environments separated by large geographic distances. Our results demonstrate this

similarity at a much finer taxonomic resolution (97% similarity) and indicate that these clades may dominate in a broad range of subseafloor sedimentary environments. Transport through the water column is far easier than through a sedimentary matrix where both advection and biologically accessible electron donors are limited.

Conclusions

Our study provides the first vertical profiles of microbial diversity from seasurface to subseafloor sediment (down to 34 mbsf). Bacterial richness is highest in the water column and lowest in the deepest sediment. The abundance-weighted communities of the water column and the subseafloor sediment are distinct from each other. Despite this difference in abundance-weighted communities, the most abundant taxa in the subseafloor sedimentary communities are generally moderately abundant in the shallow sediment communities and present but rare in the water-column communities. Our results suggest that deep subseafloor communities constitute a subset of the diverse taxa that were present in the sediment around the time of burial. However, the evolutionary processes by which these microbes get selected remains an open and intriguing avenue for future research.

Acknowledgements

We thank captain, crew and the scientific party of *R/V Knorr* Expedition 195-3 for our samples. This study was funded by the Biological Oceanography Program of the US National Science Foundation (Grant OCE- 0752336) and by the NSF-funded Center for Dark Energy Biosphere Investigations (Grant XXX-XXXXXX). This is C-DEBI

publication XXX.

References

Agogué H, Lamy D, Neal PR, Sogin ML, Herdnel GJ (2011). Water mass-specificity of bacterial communities in the North Atlantic revealed by massively parallel sequencing. *Mol Ecol* **20:** 258–274.

Baas-Becking LGM (1934). Geobiologie of inleiding tot de milieukund. *WP Van Stockum and Zoom (in Dutch): The Hague, the Netherlands*.

Behrenfeld MJ, Falkowski PG (1997). Photosynthetic rates derived from satellite-based chlorophyll concentration. *Limnol Oceanogr* **42:** 1-20.

Beman JM, Carolan MT (2013). Deoxygenation alters bacterial diversity and community composition in the ocean's largest oxygen minimum zone. *Nat Commun* **4**.

Brown MV, Philip GK, Bunge JA, Smith MC, Bissett A, Lauro FM *et al* (2009). Microbial community structure in the North Pacific Ocean. *ISME J* **3:** 1374-1386.

Bryant JA, Stewart FJ, Eppley JM, DeLong EF (2012). Microbial community phylogenetic and trait diversity declines with depth in a marine oxygen minimum zone. *Ecology* **93:** 1659-1673.

Cai P, Huang Q, Zhang X, Chen H (2006). Adsorption of DNA on clay minerals and various colloidal particles from an Alfisol. *Soil Biol Biochem* **38:** 471-476.

Caporaso GJ, Kuczynski J, Stombaugh J, Bittinger K, Bushman FD, Costello EK *et al* (2010). QIIME allows analysis of high-throughput community sequencing data. *Nature Methods* **7:** 335-336.

Clarke KR, Gorley RN (2006). PRIMER v6: User Manual/Tutorial.: PRIMER-E, Plymouth.

D'Hondt S, Jørgensen BB, Miller DJ, Batzke A, Blake R, Cragg BA *et al* (2004). Distributions of microbial activities in deep subseafloor sediments. *Science* **306:** 2216-2221.

D'Hondt S, Spivack A, Pockalny R, Ferdleman T, Fisher J, Kallmeyer J *et al* (2009). Subseafloor sedimentary life in the South Pacific Gyre. *PNAS* **106:** 11651-11656.

DeLong EF, Preston CM, Mincer T, Rich V, Hallam SJ, N. F *et al* (2006). Community genomics among stratified microbial assemblages in the ocean's Interior. *Science* **311:** 496-503.

Divins DL (2003). *Total Sediment Thickness of the World's Oceans & Marginal Seas*, vol. Boulder, CO.

Feng B-W, Li X-R, Wang J-H, Hu Z-Y, Meng H, Xiang L-Y *et al* (2009). Bacterial diversity of water and sediment in the Changjiang estuary and coastal area of the East China Sea. *FEMS Microbiol Ecol* **70:** 236-248.

Fuhrman JA, Hewson I, Schwalbach MS, Steele JA, Brown MV, Naeem S (2006). Annually reoccurring bacterial communities are predictable from ocean conditions. *PNAS* **103:** 13104-13109.

Ghiglione J-F, Galand PE, Pommier T, Pedrós-Alió C, Maas EW, Bakker K *et al* (2012). Pole-to-pole biogeography of surface and deep marine bacterial communities. *PNAS* **109:** 17633–17638.

Giovannoni SJ, Rappe MS, Vergin KL, Adair NL (1996). 16S rRNA genes reveal stratified open ocean bacterioplankton populations related to the Green Non-Sulfur bacteria. *PNAS* **93:** 7979-7984.

Gordon DA, Giovannoni SJ (1996). Detection of stratified microbial populations related to Chlorobium and Fibrobacter species in the Atlantic and Pacific oceans. *Appl Environ Microbiol* **62:** 1171-1177.

Gregg WW, Casey NW, McClain CR (2005). Recent trends in global ocean chlorophyll. *Geophys Res Lett* **32:** L03606.

Hamdan LJ, Coffin RB, Sikaroodi M, Greinert J, Treude T, Gillevet PM (2013). Ocean currents shape the microbiome of Arctic marine sediments. *ISME J* **7:** 685-696.

Hewson I, Jacobson/Meyers ME, Fuhrman JA (2007). Diversity and biogeography of bacterial assemblages in surface sediments across the San Pedro Basin, Southern California Borderlands. *Environ Microbiol* **9:** 923-933.

Hubert C, Loy A, Nickel M, Arnosti C, Baranyi C, Brüchert V *et al* (2009). A Constant Flux of Diverse Thermophilic Bacteria into the Cold Arctic Seabed. *Science* **325:** 1541-1544.

Huse SM, Dethlefsen L, Huber JA, Welch DM, Relman DA, Sogin ML (2008). Exploring microbial diversity and taxonomy using SSU rRNA hypervariable tag sequencing. *PLoS Genet* **4:** 1-10.

Inagaki F, Nunoura T, Nakagawa S, Teske A, Lever M, Lauer A *et al* (2006). Biogeographical distribution and diversity of microbes in methane hydrate-bearing deep marine sediments on the Pacific Ocean Margin. *PNAS* **103:** 2815-2820.

Jing H, Xia X, Suzuki K, Liu H (2013). Vertical Profiles of Bacteria in the Tropical and Subarctic Oceans Revealed by Pyrosequencing. *PLoS ONE* **8:** e79423.

Jørgensen BB, D'Hondt S (2006). A Starving Majority Deep Beneath the Seafloor. *Science* **314:** 932-934.

Kallmeyer J, Pockalny R, Adhikari RR, Smith DC, D'Hondt S (2012). Global distribution of microbial abundance and biomass in subseafloor sediment. *PNAS*.

Kembel SW, Eisen JA, Pollard KS, Green JL (2011). The Phylogenetic Diversity of Metagenomes. *PLoS ONE* **6:** e23214.

Ladau J, Sharpton TJ, Finucane MM, Jospin G, Kembel SW, O'Dwyer J *et al* (2013). Global marine bacterial diversity peaks at high latitudes in winter. *ISME J* **7:** 1669-1677.

Lee Y-J, Wagner ID, Brice ME, Kevbrin VV, Mills GL, Romanek CS *et al* (2005). Thermosediminibacter oceani gen. nov., sp. nov.
and Thermosediminibacter litoriperuensis sp. nov.,
new anaerobic thermophilic bacteria isolated
from Peru Margin. *Extremophiles* **9:** 375-383.

Lozupone CA, Knight R (2007). Global patterns in bacterial diversity. *PNAS* **104:** 11436-11440.

Luna GM, Dell'Anno A, Giuliano L, Danovaro R (2004). Bacterial diversity in deep Mediterranean sediments: relationship with the active bacterial fraction and substrate availability. *Environ Microbiol* **6:** 745-753.

Madrid VM, Aller JY, Aller RC, Chistoserdov AY (2001). High prokaryote diversity and analysis of community structure in mobile mud deposits off French Guiana: identification of two new bacterial candidate divisions. *FEMS Microbiol Ecol* **37:** 197-209.

Martiny JBH, Bohannan BJM, Brown JH, Colwell RK, Fuhrman JA, Green JL *et al* (2006). Microbial biogeography: putting microorganisms on the map. *Nat Rev Micro* **4:** 102-112.

Müller RD, Sdrolias M, Gaina C, Roest WR (2008). Age, spreading rates, and spreading asymmetry of the world's ocean crust. *Geochem Geophys Geosyst* **9:** Q04006.

Pommier T, Neal PR, Gasol JM, Coll M, Acinas SG, Pedrós-Alió C (2010). Spatial patterns of bacterial richness and evenness in the NW Mediterranean Sea explored by pyrosequencing of the 16S rRNA. *Aquat Microb Ecol* **61:** 221-233.

Quince C, Curtis TP, Sloan WT (2008). The rational exploration of microbial diversity. *ISME J* **2:** 997-1006.

Ravenschlag K, Sahm K, Pernthaler J, Amann R (1999). High bacterial diversity in permanently cold marine sediments. *Appl Environ Microbiol* **65:** 3982–3989.

Røy H, Kallmeyer J, Adhikari RR, Pockalny R, Jørgensen BB, D'Hondt S (2012). Aerobic microbial respiration in 86-million year old deep-sea red clay. *Science* **336:** 922-925.

Schauer R, Bienhold C, Ramette A, Harder J (2010). Bacterial diversity and biogeography in deep-sea surface sediments of the South Atlantic Ocean. *ISME J* **4:** 159-170.

Sogin M, Morrison H, Welch D, Huse S, Neal P, Arrieta J *et al* (2006). Microbial diversity in the deep-sea and the unexplored "rare Biosphere". *PNAS* **103:** 12115-12120.

Treusch AH, Vergin KL, Finlay LA, Donatz MG, Burton RM, Carlson CA *et al* (2009). Seasonality and vertical structure of microbial communities in an ocean gyre. *ISME J* **3:** 1148-1163.

Wright TD, Vergin KL, Boyd PW, Giovannoni SJ (1997). A novel d-subdivision proteobacterial lineage from the lower ocean surface layer. *Appl Environ Microbiol***:** 1441-1448.

Zinger L, Amaral-Zettler LA, Furhman JA, Horner-Devine MC, Huse SM, Welch DBM *et al* (2011). Global patterns of bacterial beta-diversity in seafloor and seawater ecosystems. *PLoS One* **6**.

Tables

Sample ID	Location	Depth (m)	# of Reads	PD	Chao1 (97%)	OTUs (97%)	Evenness (97%)	Oxygen (mmol/kg)	Chorophyll (mg/m3)	AOU (umol/kg)
EQP 1 (3 m)	EQP 1	3	4666	61	863.312	482.6	0.6588	201.066	0.6061	6.889
EQP 1 (34 m)	EQP 1	34	4666	56.835	958.861	505.6	0.7223	101.738	1.075	136.477
EQP 1 (101 m)	EQP 1	101	4666	75.566	1460.96	808.8	0.7829	92.84	0.3452	159.149
EQP 1 (150 m)	EQP 1	150	4666	67.987	1047.54	699.9	0.8085	44.982	0.2443	210.547
EQP 1 (200 m)	EQP 1	200	4666	69.637	706.283	536.2	0.804	54.816	0.2243	202.607
EQP 1 (249 m)	EQP 1	249	4666	82.215	1669.8	850.8	0.7767	21.223	0.1998	241.257
EQP 1 (299 m)	EQP 1	299	4666	93.819	2330.47	950	0.7654	6.382	0.2184	263.787
EQP 1 (348 m)	EQP 1	348	4666	80.437	1631.22	827.7	0.7437	6.158	0.2188	268.446
EQP 1 (774 m)	EQP 1	774	4666	81.307	1600.68	811.3	0.7525	43.057	0.1954	259.619
EQP 1 (991 m)	EQP 1	991	4666	72.432	1214.01	736.9	0.7596	51.894	0.1875	257.583
EQP 1 (1485 m)	EQP 1	1485	4666	76.978	1248.02	719.9	0.7521	73.208	0.1851	248.773
EQP 1 (1978 m)	EQP 1	1978	4666	70.946	901.399	600.6	0.7644	91.723	n/a	236.85
EQP 1 (2500 m)	EQP 1	2500	4666	71.489	882.767	584.3	0.753	95.981	n/a	236.31
EQP 1 (2832 m)	EQP 1	2832	4666	68.54	823.605	565.1	0.7847	97.211	n/a	236.52
EQP 8 (2 m)	EQP 8	2	4666	77.864	2792.52	772.3	0.6889	188.246	0.4324	18.01
EQP 8 (41 m)	EQP 8	41	4666	92.75	3847.19	949.2	0.7058	181.479	1.065	27.692
EQP 8 (142 m)	EQP 8	142	4666	191.099	10682.2	2176.1	0.8602	123.659	0.1812	105.382
EQP 8 (442 m)	EQP 8	442	4666	129.601	5219.29	1371.8	0.7934	30.062	0.1581	249.43
EQP 8 (998 m)	EQP 8	998	4666	115.599	4172.81	1197.9	0.7707	84.482	0.135	227.337
EQP 8 (1980 m)	EQP 8	1980	4666	103.987	2924.85	968.4	0.7515	102.425	0.0482	226.57
EQP 8 (4296 m)	EQP 8	4296	4666	127.211	3692.32	1152.1	0.7384	154.366	0.0738	181.988
EQP 11 (3 m)	NPG	3	4666	86.152	2429.13	837.3	0.6816	211.787	0.1792	12.92
EQP 11 (127 m)	NPG	127	4666	102.13	3107.82	1007.5	0.7122	211.874	0.1375	12.79
EQP 11 (600 m)	NPG	600	4666	152.416	5674.87	1594.7	0.8156	125.057	0.0521	173.53
EQP 11 (900 m)	NPG	900	4666	182.803	6551.62	1911.6	0.8453	18.947	0.069	296.935
EQP 11 (1981 m)	NPG	1981	4666	157.486	5301.15	1611.2	0.8196	70.345	0.0524	260.944
EQP 11 (3955 m)	NPG	3955	4666	80.76	1306.08	632.1	0.7087	135.545	0.0348	200.91
EQP 11 (5816 m)	NPG	5816	4666	86.151	1498.35	668.1	0.7396	148.297	0.0348	186.294

Table 1: Sampling information and diversity estimates for water and sediment collected from three different sites in located in the eastern, central and north Pacific Ocean. Diversity estimates were generated from 16S rRNA 454 pyrosequencing data after sub-sampling down to the lowest number of reads.

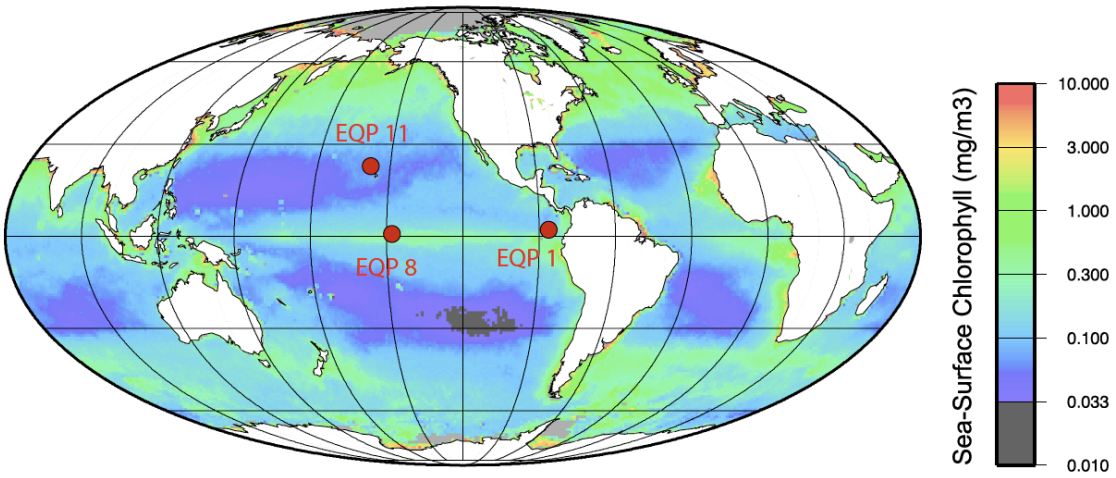

Figure 1: Locations of sampling stations. Superimposed chlorophyll *a* content was a collected annual average (mean from September 1994-December 2004) from SeaWiFS satellite data that was uploaded into GeoMapApp (Behrenfeld and Falkowski, 1997; Gregg et al., 2005; Ryan et al., 2009).

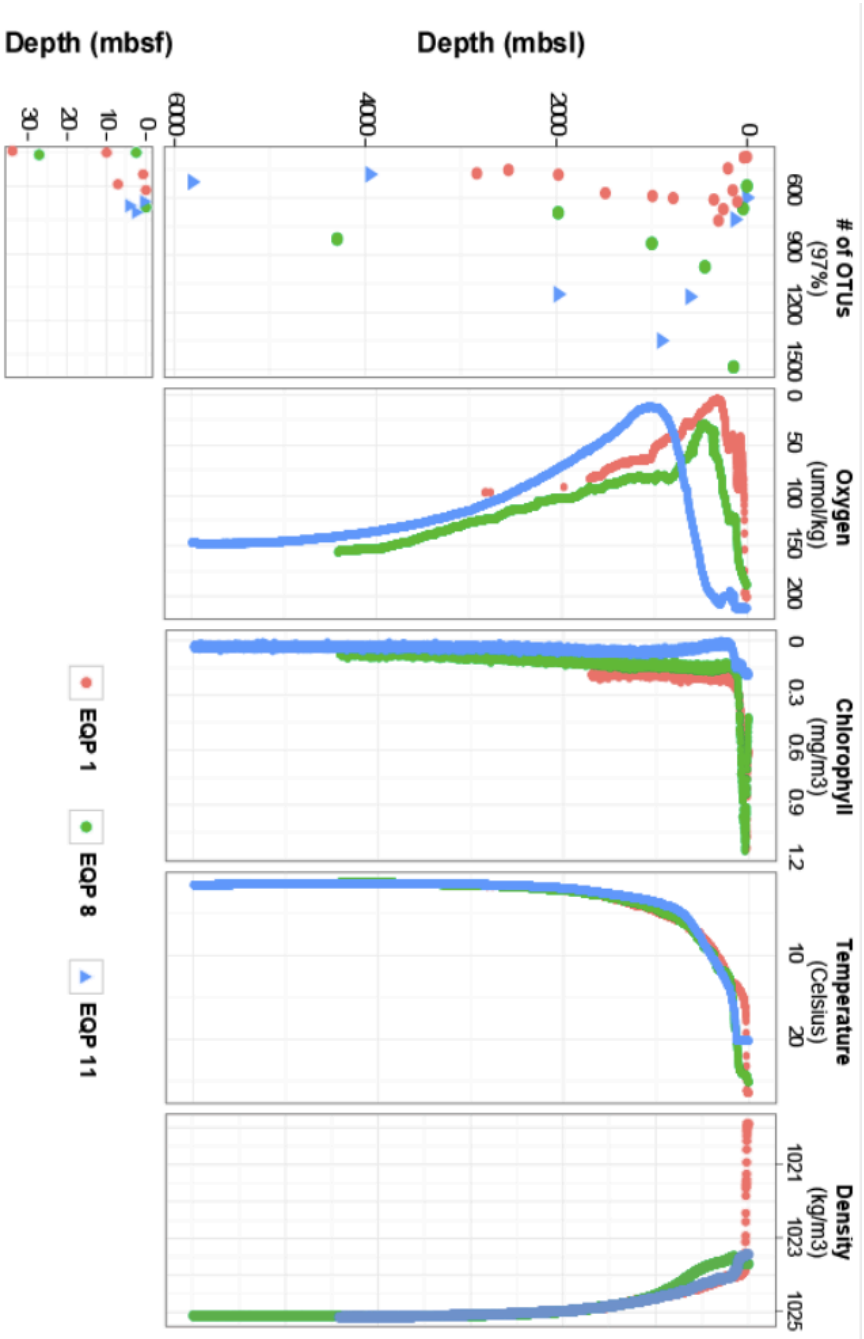

Figure 2: Scatterplot of sequencing and CTD data including (A) CHAO-1, (B) oxygen, (C) chlorophyll a, (D) temperature and (E) density.

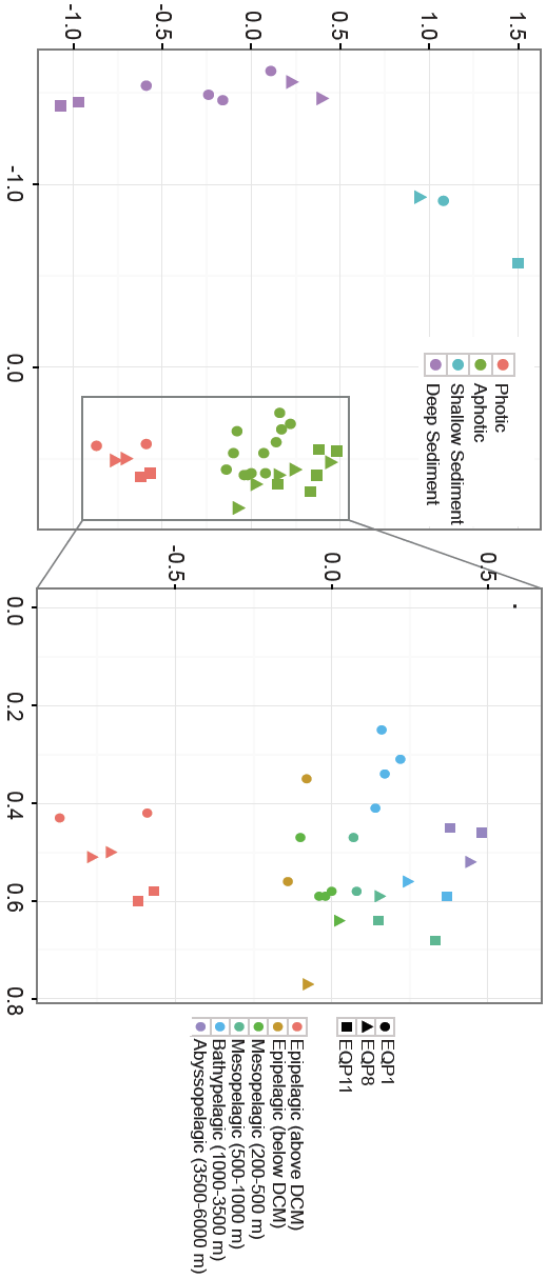

Figure 3: (A) Non-metric multidimensional scaling plot of both the water column and subseafloor sediment communities based upon Bray-Curtis similarities indices. (B) Non-metric multidimensional scaling plot of the water column communities with a superimposed depth gradient from seasurface (red) to the abyssopelagic water of EQP8 and EQP11 (blue).

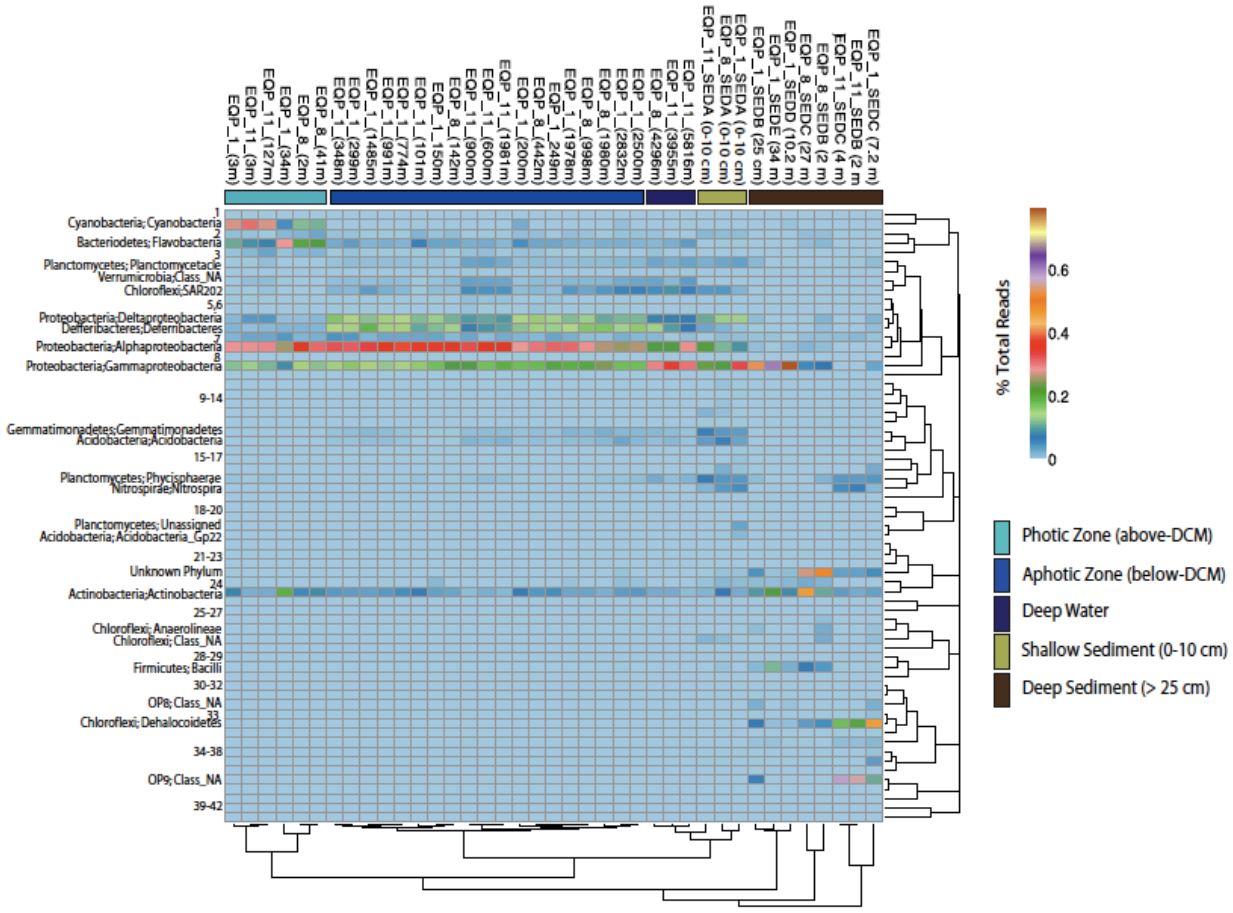

Figure 4: Heatmap clustering visualization of water column and sediment bacterial communities (x-axis) and class-level GAST taxonomy (y-axis). The heatmap was color coded by the percent a given taxon is contributing to any given sample. Hierarchal clustering was based on the Morista-Horn similarity index.

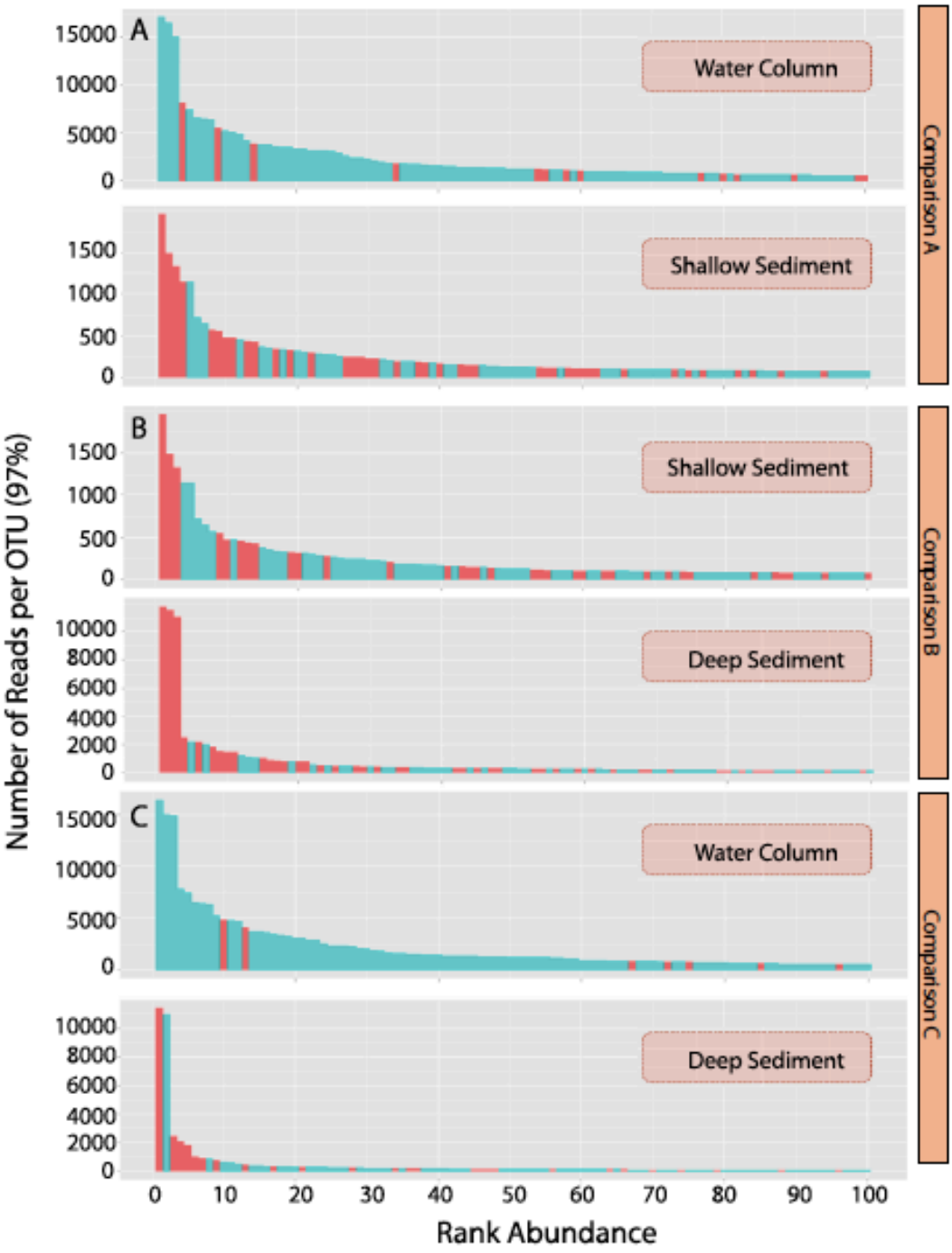
A
Water Column
Shallow Sediment
B
Shallow Sediment
Deep Sediment
C
Water Column
Deep Sediment
Comparison A
Comparison B
Comparison C
Number of Reads per OTU (97%)
Rank Abundance
0
10
20
30
40
50
60
70
80
90
100

Figure 5: Rank abundance histograms examining the community overlap between the water column and shallow sediment (comparison A), shallow sediment and deep sediment (≥2m) (comparison B), and the water column and deep sediment (≥2m)(comparison C). Operational Taxonomic Units (OTUs) highlighted in pink were shared between compared environments, while blue indicates that it was unique.

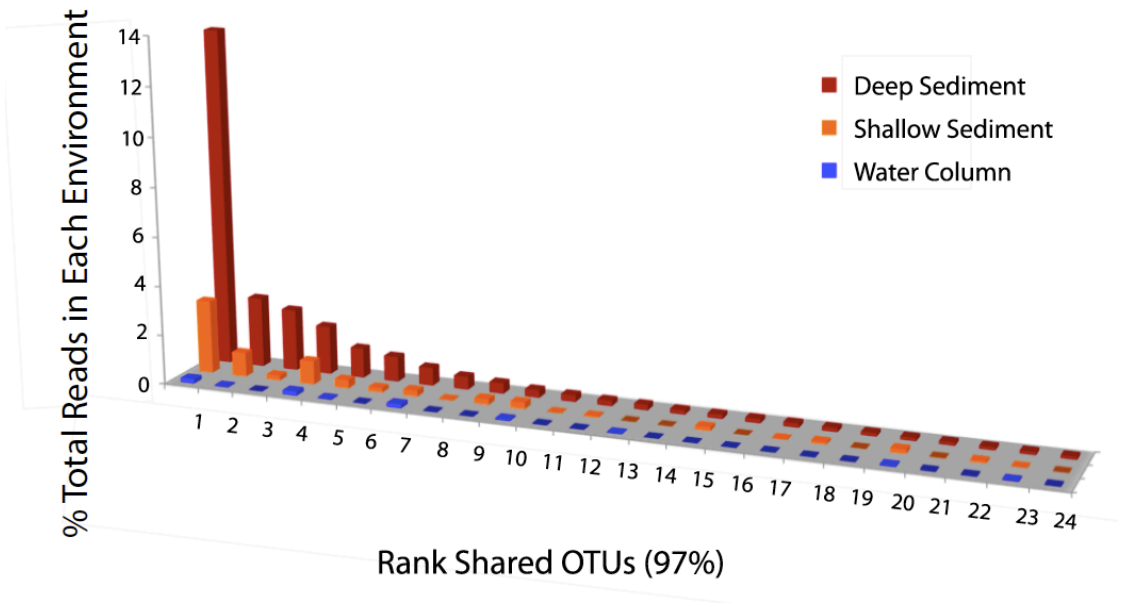

Figure 6: Rank abundance histograms for the top OTUs shared (x-axis) between the oceanic and sedimentary environment. The y-axis indicates the percent of the total number of reads per OTU within our subseafloor sediment samples (≥ 2 mbsf, red), shallow sediment samples (orange) and water column samples (blue).

MANUSCRIPT III

BACTERIAL DIVERSITY, SEDIMENT AGE AND ORGANIC RESPIRATION IN THE MARINE SEDIMENTARY ENVIRONMENT

By

Emily Walsh[1], John Kirkpatrick[1], Robert Pockalny[1], Justine Sauvage[1], Mitchell Sogin[2], Steven D'Hondt[1]

[1] Graduate School of Oceanography, University of Rhode Island, Narragansett Bay Campus, 215 South Ferry Road, Narragansett, RI 02882, USA

[2]Josephine Bay Paul Center for Comparative Molecular Biology and Evolution, Marine Biological Laboratory, 7 MBL Street, Woods Hole, MA 02543, USA

To be submitted to Nature 2014

Subseafloor sediment hosts to a large[1], taxonomically rich[2] and metabolically diverse[3] microbial ecosystem. However, the factors that control microbial diversity in subseafloor sediment have rarely been explored. Here we show that subseafloor bacterial richness varies directly with net rate of organic-fueled respiration and sediment age. We examined three open-ocean sites (in the Bering Sea and equatorial Pacific) and one continental margin site (Indian Ocean), with sediment depths to 404 meters below seafloor. At all locations, taxonomic richness decreases exponentially with increasing sediment depth. This profile generally matches the canonical relationship between rates of organic oxidation and sediment depth and age[4,5]. To examine the potential link between organic oxidation and taxonomic richness we used pore-water chemical profiles to quantify net rates of organic respiration at the three open-ocean sites (the chemical profiles of the ocean-margin site are not in diffusive steady state). Taxonomic richness and total rate of organic-fueled respiration are highest at the high productivity Bering Sea site and lower at the moderate productivity equatorial Pacific sites. At each of these sites, organic-fueled respiration rate and taxonomic richness are highest at the surface and decline together as sediment depth and age increase. Transformation of sediment depth to sediment age demonstrates that richness declines most rapidly for a few hundred thousand years after sediment deposition. To our knowledge, this is the first evidence that taxonomic richness is closely linked to organic-fueled respiration rate and sediment age in subseafloor sediment.

Subseafloor sediment contains a highly diverse microbial world with total cell abundance comparable to that in terrestrial soil and in the world ocean[1]. Subseafloor communities push the boundaries of life as we know it; their per-cell rates of respiration are often orders of magnitude lower than in the surface world[6] they take hundreds of years to turn over their biomass[7,8] and microbes in deep subseafloor sediment may be isolated from the surface world for myrs to tens of myrs. Subseafloor

sediment, therefore, provides an unprecedented opportunity to investigate the driver(s) of microbial diversity in a natural laboratory over a geologic time scale.

To document microbial diversity and its potential drivers in subseafloor sediment, we extracted and pyrosequenced the v4-v6 hyper-variable region of the bacterial 16S rRNA gene from sediment recovered at four very different locations: the Bering Sea [Integrated Ocean Drilling Program (IODP) Expedition 323 Site U1343][9], the eastern equatorial Pacific (Knorr expedition 195-3 Site EQP-1), the central equatorial Pacific Ocean (Knorr 195-3 Site EQP8) and the Bengal continental margin [Indian National Gas Hydrate Program (NGHP) Site NGHP-1-14][10]. Three of these sites are in the open ocean [U1343, EQP1 and EQP8, at water depths of 1953, 2885 and 4336 meters below sealevel (mbsl), respectively] and the fourth, continental margin Site NGHP-1-14, is at 895 mbsl (NGHP-1-14) (Fig. 1a).

The Bering Sea and Bay of Bengal sites are characterized by high-productivity surface water and very high sedimentation rates (0.94 and 0.32 mg/m^3 and, 100 and 250 m/Ma at NGHP-1-14 and U1343, respectively); while the equatorial Pacific sites are characterized by moderate productivity and moderate mean sedimentation rates (0.21 and 0.15 mg/m^3 and, 4.75 and 75 m/Ma at EQP8 and EQP1, respectively). Total organic carbon (TOC) content of surface sediment is highest at the high sedimentation sites (0.6% and 1.7% at NGHP-1-14 and U1343, respectively) and lowest at the moderate sedimentation sites (0.02 and 0.1% at EQP8 and EQP1, respectively). Maximum sampled sediment depths range from 27 meters below seafloor (mbsf) at equatorial Pacific site EQP8 to 404 mbsf at Bering Sea Site U1343 (Supplementary Table 1). Concentration profiles of dissolved metabolic products [inorganic carbon

(DIC), methane, ammonium], dissolved metabolic reactants (oxygen, nitrate, sulfate) indicate that microbial activity occurs throughout the sampled sediment sequences, but declines with increasing sediment depth[11,12].

Previous studies using the 16S rRNA gene [13-15] or 16S rRNA itself[16] have shown that subseafloor sedimentary community composition varies with the availability of dissolved metabolic reactants (e.g., oxygen, sulfate, methane). Most such studies have focused on the subseafloor sulfate/methane transition zone (SMTZ), and found the bacterial[13,15] and/or archaeal[15,16] community composition of that zone to be distinct from the communities of the overlying sulfate-replete sediment and the underlying methane-replete, sulfate-poor sediment. Given these differences in community composition, availability of dissolved metabolic reactants might conceivably also drive subseafloor variation in taxonomic richness (the number of taxa present in each sample).

To test this possibility, we compare both abundance-weighted community composition and taxonomic richness to dissolved water chemistry at all four of our sites. Our community composition results agree with previous studies by showing abundance-weighted community composition to vary significantly with the availability of dissolved metabolic reactants ($p=0.002$) (Fig. 1b). Our abundance-weighted (Bray-Curtis) similarity scores[17] exhibit a clear gradient through the following vertical sequence of dissolved chemical zones[18]: (i) the oxygenated zone immediately beneath the seafloor, (ii) a deeper zone with abundant dissolved sulfate, (iii) a still deeper sulfate/methane SMTZ, and (iv) the deepest zone, with little or no dissolved sulfate but abundant dissolved methane (Fig. 1b).

Despite its effect on community composition, dissolved water chemistry does not drive taxonomic richness. Bacterial taxonomic richness is highest near the seafloor and drops to lower values with increasing sediment depth (Fig. 2). The rate of decrease in richness with depth varies greatly from site to site, but is not associated with any particular geochemical zone or transition between zones. This exponential decline in richness occurs at multiple phylogenetic levels (Extended Data Fig. 1); the number of species (97%), genera (95%), families (~92%) and phyla (~80%) all decline with increasing sediment depth.

This exponential decline in taxonomic richness generally matches the canonical relationship between sediment depth and TOC, the principle food source for the subseafloor sedimentary biosphere[3]. Often described with a Multi-G model, which interprets TOC as comprised of multiple kinds of organic matter with varying degrees of reactivity or biological accessibility. In this model, the most labile or biologically reactive organic substrates are respired at much faster rates than the least labile substrates, leading the net rates of organic-fueled respiration to decrease exponentially with sediment depth[4].

To quantify net rates of organic-fueled respiration, we modeled pore-water chemical profiles (DIC and ammonium) using a finite-based solutions model[19]. This model could not be applied to the continental margin site NGHP-1-14 as it is not in diffusive steady state. At site U1343, we limited the modeling of DIC production rates to the upper sediment column (<90 mbsf)(Extended Data Figure 3), due to evidence of DIC consumption and carbonate formation at greater depths (between 300 and 384 mbsf

)[12]. We also modeled net ammonium production rates for this site, in order to calculate rates of reaction for the entire sediment column (Fig.3A).

At the open-ocean sites (U1343, EQP1 and EQP8) the rate of organic-fueled respiration is highest near the seafloor with higher activity corresponding with higher taxonomic richness (Fig. 3 A,B). As expected from the Multi-G model, net rates of organic-fueled respiration and taxonomic richness decline along with increasing sediment depth (Fig. 3A,B). The reactivity of organic carbon has also been demonstrated to decline not only with depth but also as a function of time[5]. Transformation of sediment depth to sediment age shows that taxonomic richness decreases exponentially with age at all four sites (Fig. 4); it decreases rapidly during the first few hundred thousand years and then stabilizes or decreases more slowly with greater age (Fig. 4). These results support our claim that taxonomic richness in the deep subseafloor is interconnected to net rates of organic respiration and sediment age; ultimately driven by the bioavailability of TOC.

Methods

Shipboard sampling and geochemistry

Immediately after core recovery, we cut sediment cores into Whole Round Cores (WRC) for Interstitial Water (IW) analysis. Immediately after cutting a WRC for IW analyses, we cleaned the cut face of the remaining core section with a sterile blade, and then took one to four samples for DNA analyses from the center of the cleaned core face using sterile 60 cm^3 syringes from which the Luer end had been cut off. We froze the syringe samples at -80 °C for shore-based DNA analysis. Interstitial water chemistry was characterized shipboard according to standard procedures[3,9,20].

Pyrosequencing, clustering and OTU identification

We amplified the v4-v6 hypervariable region of the 16S rRNA gene using a master mix containing 2 μl PFU Ultra II polymerase, 10x PFU buffer, 10 μM dNTPs, de-ionized water and 25 μM bacterial primers 518f-1064r in a 25 ul reaction volume. Thermocycling conditions were as follows: 94°C for 3 min, 30 cycles of 94°C for 30 s, 57°C for 45 s and 72°C for 1 min, and a final 72°C extension step for 2 min. We purified amplicons using the Agencourt AMPure XP system and pooled them in triplicate to avoid PCR-induced error. We sequenced pooled PCR products following standard protocols on a 454 GS-FLX sequencer at the Josephine Bay Paul Center, Marine Biological Laboratory, Woods Hole, MA. To reduce error, we removed low-quality sequences prior to analysis. These low-quality sequences included (i) reads that contained an ambiguous base (n) ,(ii) reads that had no match to 5-nt key or primer set, and (iii) reads that were less than 500 bp in length. This trimming protocol is described in detail by Huse et al. 2007[21]. To determine the taxonomy of each sample at the Genus level, we used the GAST system for sequence identification (www.vamps.mbl.edu), based on the SILVA database. From EQP-1 samples, we removed all sequences that correspond to the taxon *Vibrio*, because *Vibrio* was actively cultured in the laboratory used for EQP-1 DNA extraction; no *Vibrio* DNA occurs in samples from the other sites, which were extracted in a laboratory dedicated to this project. We used the QIIME[22] pipeline to cluster each sample into OTUs at the 3% similarity-level. To investigate patterns in diversification with depth samples were also clustered at multiple levels of similarity to generate lineage through time plots.

Statistical Analyses

To remove any effects of sample size on down-hole or inter-site comparisons of taxonomic richness and Chao-1 estimates, we used the program Qiime[22] to randomly reduce (daisy chop) the number of reads in each sample to the lowest number of reads in any single sample. However, the observed declines in diversity with sediment depth and age are robust even at much less rigorous levels of sub-sampling [e.g., in comparison of samples that vary in total read number by up to 3x (data not shown)]. We performed Bray-Curtis similarity analyses, non-metric multidimensional scaling and Spearman rank correlation tests using the Primer 6 program[23].

Modeling Rates of Reaction

Prior to analysis, measurements for DIC (Extended Data Fig.2) and Alkalinity were corrected for sampling artifacts[24]. Rates of reaction were performed using a modified version of the wang et al. model[19]. This modification includes the use of a chemospline, instead of a 5-point running mean, in order to generate a best-fit line to the measured DIC data.

References

1 Kallmeyer, J., Pockalny, R., Adhikari, R. R., Smith, D. C. & D'Hondt, S. Global distribution of microbial abundance and biomass in subseafloor sediment. *Proceedings of the National Academy of Sciences*, doi:10.1073/pnas.1203849109 (2012).

2 Inagaki, F. *et al.* Biogeographical distribution and diversity of microbes in methane hydrate-bearing deep marine sediments, on the Pacific Ocean Margin. *Proceedings of the National Academy of Sciences* **103**, 2815-2820 (2006).

3 D'Hondt, S. *et al.* Distributions of Microbial Activities in Deep Subseafloor Sediments. *Science* **306**, 2216-2221, doi:10.1126/science.1101155 (2004).

4 Jorgensen, B. B. A comparison of methods for the quantification of bacterial sulfate reduction in coastal marine sediments. *Geomicrobiology Journal* **1**, 49-64, doi:10.1080/01490457809377723 (1978).

5 Middelburg, J. J. A simple rate model for organic matter decomposition in marine sediments. *Geochimica et Cosmochimica Acta* **53**, 1577-1581, doi:http://dx.doi.org/10.1016/0016-7037(89)90239-1 (1989).

6 Hoehler, T. M. & Jorgensen, B. B. Microbial life under extreme energy limitation. *Nat Rev Micro* **11**, 83-94 (2013).

7 Lomstein, B. A., Langerhuus, A. T., D/'Hondt, S., Jorgensen, B. B. & Spivack, A. J. Endospore abundance, microbial growth and necromass turnover in deep sub-seafloor sediment. *Nature* **484**, 101-104, doi:http://www.nature.com/nature/journal/v484/n7392/abs/nature10905.html#supplementary-information (2012).

8 Biddle, J. F. *et al.* Heterotrophic Archaea dominate sedimentary subsurface ecosystems off Peru. *PNAS* **103**, 3846-3851, doi:doi:10.1073/pnas.0600035103 (2006).

9 Expedition 323 Scientists. Bering Sea paleoceanography: Pliocene–Pleistocene paleoceanography and climate history of the Bering Sea. *IODP preliminary report 323*, doi:doi:10.2204/iodp.sp.323.2009 (2010).

10 Collett, T. *et al.* (Directorate General of Hydrocarbons,Ministry of Petroleum and Natural Gas (India), Mumbai, India, 2006).

11 Schrum, H. N., Spivack, A. J., Kastner, M. & D'Hondt, S. Sulfate-reducing ammonium oxidation: A thermodynamically feasible metabolic pathway in subseafloor sediment. *Geology* **37**, 939-942, doi:10.1130/g30238a.1 (2009).

12 Wehrmann, L. M. *et al.* Coupled organic and inorganic carbon cycling in the deep subseafloor sediment of the northeastern Bering Sea Slope (IODP Exp. 323). *Chemical Geology* **284**, 251-261, doi:http://dx.doi.org/10.1016/j.chemgeo.2011.03.002 (2011).

13 Parkes, R. J. *et al.* Deep sub-seafloor prokaryotes stimulated at interfaces over geological time. *Nature* **436**, 390-394, doi:http://www.nature.com/nature/journal/v436/n7049/suppinfo/nature03796_S1.html (2005).

14 Fry, J. C., Webster, G., Cragg, B. A., Weightman, A. J. & Parkes, R. J. Analysis of DGGE profiles to explore the relationship between prokaryotic community composition and biogeochemical processes in deep subseafloor sediments from the Peru Margin. *FEMS Microbiology Ecology* **58**, 86-98, doi:10.1111/j.1574-6941.2006.00144.x (2006).

15 Harrison, B. K., Zhang, H., Berelson, W. & Orphan, V. J. Variations in Archaeal and Bacterial Diversity Associated with the Sulfate-Methane Transition Zone in Continental Margin Sediments (Santa Barbara Basin, California). *Applied and Environmental Microbiology* **75**, 1487-1499, doi:10.1128/AEM.01812-08 (2009).

16 Sørensen, K. B. & Teske, A. Stratified Communities of Active Archaea in Deep Marine Subsurface Sediments. *Applied and Environmental Microbiology* **72**, 4596-4603 (2006).

17 Bray, J. R. & Curtis, J. T. An ordination of upland forest communities of southern Wisconsin. *Ecological Monographs* **27**, 325-349 (1957).

18 Froelich, P. N. *et al.* Early oxidation of organic matter in pelagic sediments of the eastern equatorial Atlantic: suboxic diagenesis. *Geochimica et Cosmochimica Acta* **43**, 1075-1090 (1979).

19 Wang, G., Spivack, A. J., Rutherford, S., Manor, U. & D'Hondt, S. Quantification of co-occurring reaction rates in deep subseafloor sediments. *Geochimica et Cosmochimica Acta* **72**, 3479-3488, doi:http://dx.doi.org/10.1016/j.gca.2008.04.024 (2008).

20 Gieskes, J. M., Gamo, T. & Brumsack, H. Chemical methods for interstitial water analysis aboard JOIDES Resolution. *ODP Technical Note* **15**, doi:http://wwwodp.tamu.edu/publications/tnotes/tn15/ f_chem1.htm (1991).
21 Huse, S., Huber, J., Morrison, H., Sogin, M. & Welch, D. Accuracy and quality of massively parallel DNA pyrosequencing. *Genome Biology* **8**, R143 (2007).
22 Caporaso, G. J. *et al.* QIIME allows analysis of high-throughput community sequencing data. *Nature Methods* **7**, 335-336, doi: 10.1038/nmeth.f.303 (2010).
23 PRIMER v6: User Manual/Tutorial. (PRIMER-E, Plymouth, 2006).
24 Sauvage, J., Spivack, A. J., Murray, R. W. & S., D. H. Reconstruction of in-situ dissolved inorganic carbon concentration and alkalinity in marine sedimentary pore water. *American Geophysical Union, Fall Meeting* **Abstract PP31B-1858** (2011).

Supplementary Information is linked to the online version of the paper at www.nature.com/nature.

Acknowledgements

This research would not have been possible without the dedicated effort of the crews and scientific staff of the Drillship *JOIDES Resolution* and the Research Vessel *Knorr*. The samples were provided by Indian National Gas Hydrates Program Expedition 01, Expedition *Knorr* 195-III, and Integrated Ocean Drilling Program Expedition 323. The post-expedition analyses were funded by the U.S. National Science Foundation [through the NSF Biological Oceanography Program (grant OCE-0752336) and the Center for Dark Energy Biosphere Investigations (C-DEBI)] and by the Sloan Foundation (through the Deep Carbon Observatory Census of Deep Life). This is C-DEBI publication XXX.

Author Contributions

E.A.W. and S.D. designed the study. E.A.W. and J.B.K. processed the samples. R.P. modeled the reaction rates using data corrected by J.S. M.L.S. oversaw the pyrosequencing effort. E.A.W., J.B.K., M.L.S. and S.D. analyzed data. E.A.W. wrote

the manuscript with significant input from J.B.K., M.L.S. and S.D.

Author Information

All sequencing results for this study can be accessed and visualized online at www.vamps.mbl.edu All environmental data for Site U1343 are deposited in the IODP database and accessible on-line in the IODP Expedition 323 Proceedings. All environmental data for Sites EQP1 and EQP8 are deposited in the BIO-DMO database. Reprints and permission information are available at www.nature.com/reprints. We report no competing financial interests. Correspondence and requests for materials should be addressed to E.W. (ewalsh@gso.uri.edu).

Figure Legends

Figure 1: Map of sampling locations (A). Non-Metric Multidimensional Scaling (nMDS) plot (B). Bray-Curtis distances between samples were representative of the degree of community similarity where samples containing similar communities are positioned closer together in ordination space (stress=0.01). Color indicates geochemical zone and shape indicates site location.

Figure 2: Filled circles, OTUs; open squares Chao-1 richness index (citation). Dark grey shading indicates oxygen penetration depth, light grey shading indicates the presence of sulfate and an absence of color indicates sulfate is below detection.

Figure 3: (A) Net ammonium and DIC production rates were calculated for Bering Sea site U1343, while (B) net DIC-corrected production rates were calculated for equatorial Pacific sites EQP 1 and EQP8 using a modified version of the Wang model[19]. Standard deviation was determined through the use of a Monte Carlo

simulation (n=30) and considered significant if the upper and lower limit resided above zero. Significant production rates are represented by the gray bars and OTUs (97%) by the blue circles.

Figure 4: OTUs plotted against sediment age. Shape indicates site location.

Supplementary Table

Extended Data Table 1: Environmental and sampling data collected for each of the four sampling locations.

Supplementary Figures

Extended Data Figure 1: Lineage through time (LTT) plot for the Bering Sea site U1343. The x-axis indicates clustering level (0-18%) and the y-axis indicates the number of OTUs generated. Trend was replicated at the remaining three sites (EQP1, EQP8 and NGHP-1-14) (data not shown).

Extended Data Figure 2: Measured shipboard DIC (red stars) and corrected DIC (blue squares) for sites EQP1 and EQP8.

Extended Data Figure 3: Measured ammonium and DIC for Bering Sea site U1343.

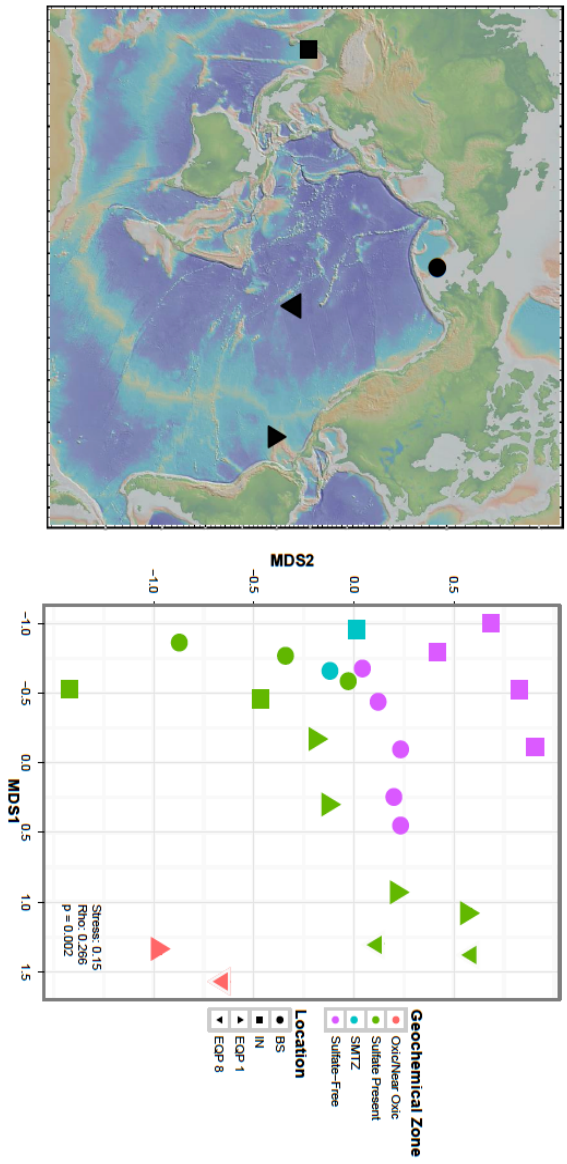

Figure 1: Map of sampling locations (A). Non-Metric Multidimensional Scaling (nMDS) plot (B). Bray-Curtis distances between samples were representative of the degree of community similarity where samples containing similar communities are positioned closer together in ordination space (stress=0.01). Color indicates geochemical zone and shape indicates site location.

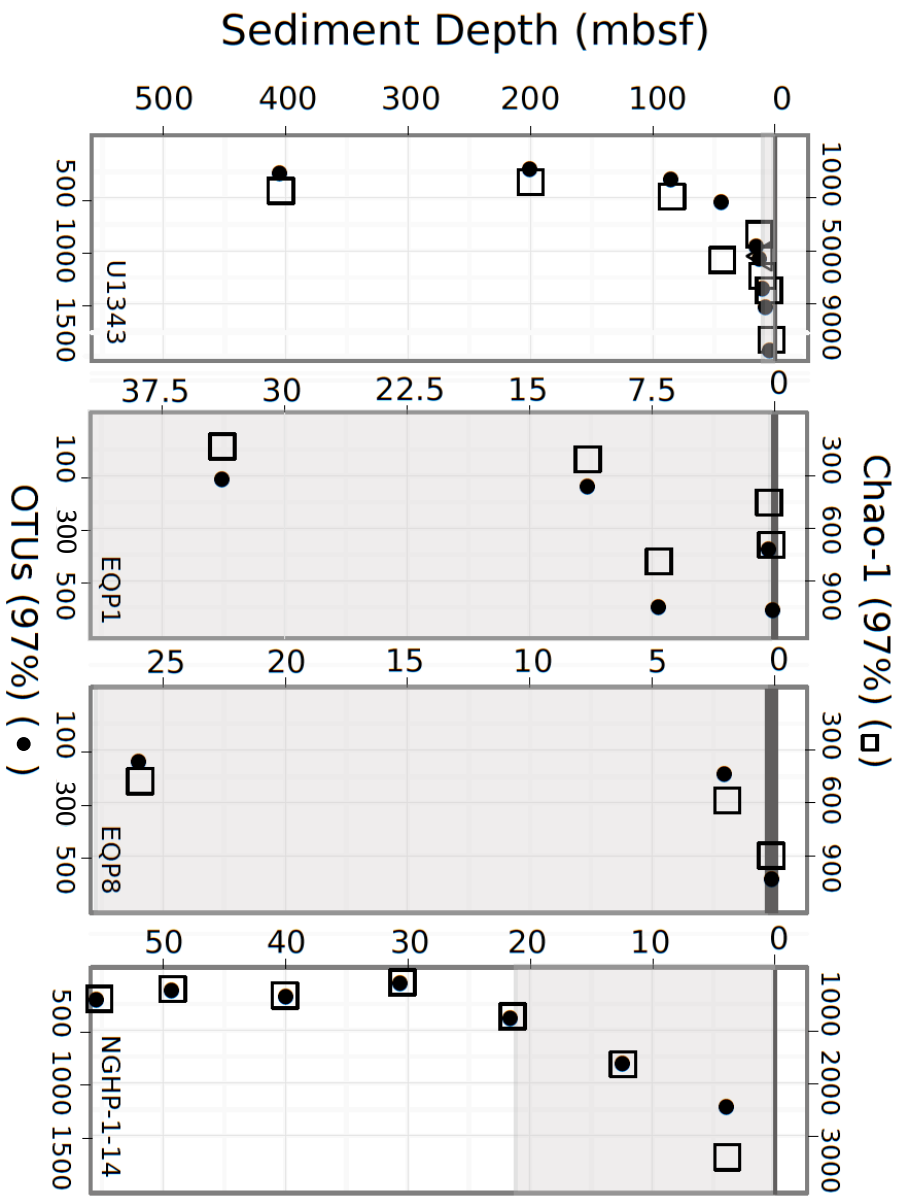

Figure 2: Filled circles, OTUs; open squares Chao-1 richness index (citation). Dark grey shading indicates oxygen penetration depth, light grey shading indicates the presence of sulfate and an absence of color indicates sulfate is below detection.

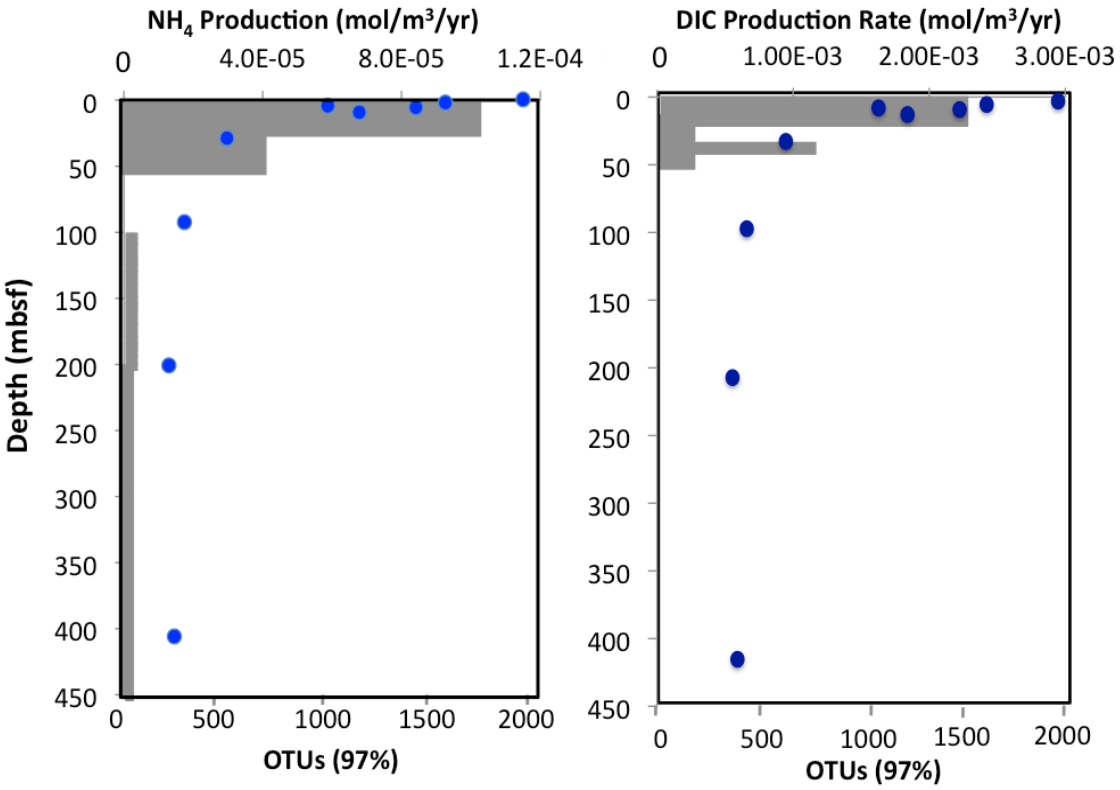
NH4 Production (mol/m3/yr)
0
4.0E-05
8.0E-05
1.2E-04
DIC Production Rate (mol/m3/yr)
0
1.00E-03
2.00E-03
3.00E-03
Depth (mbsf)
0
50
100
150
200
250
300
350
400
450
0
500
1000
1500
2000
OTUs (97%)

B

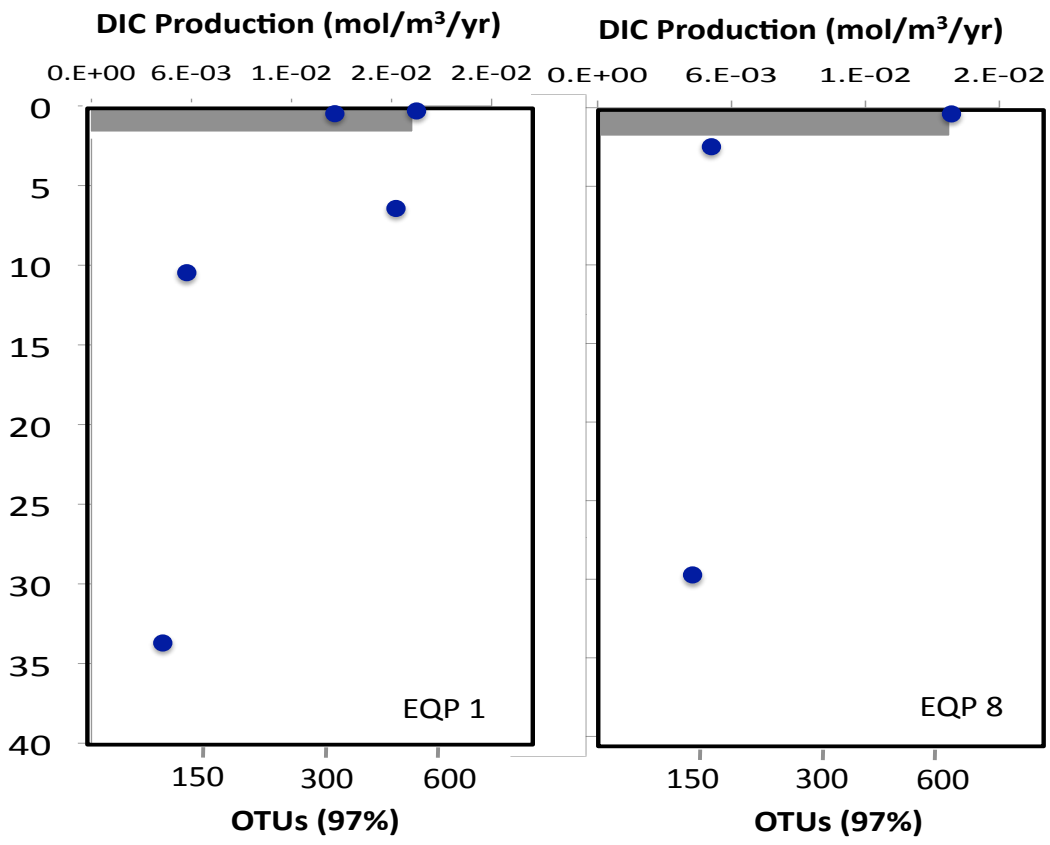
DIC Production (mol/m3/yr)
0.E+00
6.E-03
1.E-02
2.E-02
2.E-02
DIC Production (mol/m3/yr)
0.E+00
6.E-03
1.E-02
2.E-02
0
5
10
15
20
25
30
35
40
EQP 1
EQP 8
150
300
600
OTUs (97%)

Figure 3: (A) Net ammonium and DIC production rates were calculated for Bering Sea site U1343, while (B) net DIC-corrected production rates were calculated for equatorial Pacific sites EQP 1 and EQP8 using a modified version of the Wang model[19]. Standard deviation was determined through the use of a Monte Carlo simulation (n=30) and considered significant if the upper and lower limit resided above zero. Significant production rates are represented by the gray bars and OTUs (97%) by the blue circles.

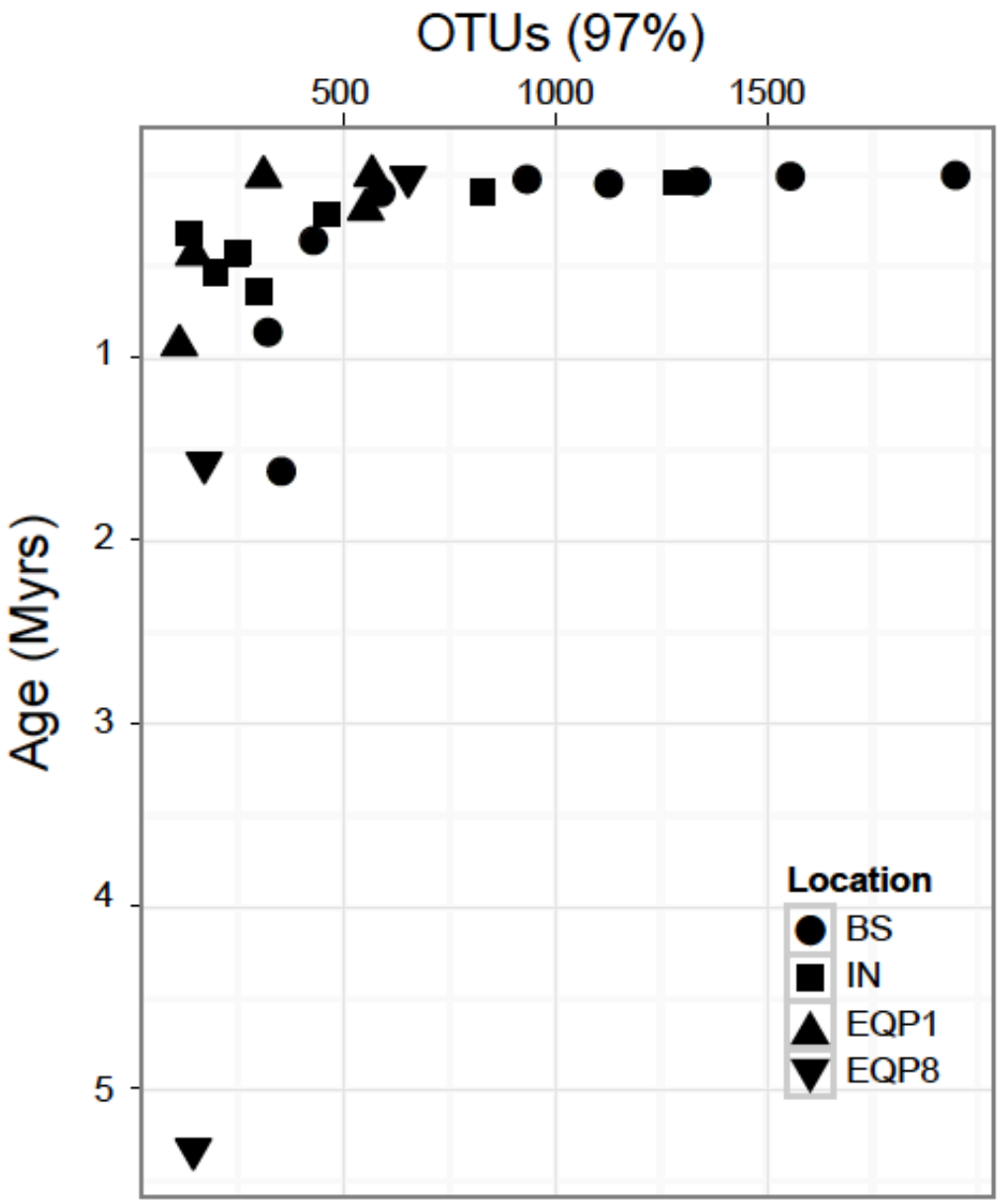

Figure 4: OTUs plotted against sediment age. Shape indicates site location.

Tables

Sample ID	Latitude	Longitude	Water Depth (m)	Sample Depth (mbsf)	Age (yrs)	TOC (wt%)	Sulfate (mM)	TON (wt%)	C:N Ratio	Cells (log10/g)
BS1	57°33.3993′N	175°48.9659′W	1953	0.15	600	1.14	25.85	0.13	8.83	7.6
BS2	57°33.3993′N	175°48.9659′W	1953	1.65	6600	0.84	20.85	0.10	8.13	6.2
BS3	57°33.3993′N	175°48.9659′W	1953	5.65	22600	0.93	11.88	0.10	8.91	6.2
BS4	57°33.3993′N	175°48.9659′W	1953	8.65	34600	0.80	0.00	0.22	3.56	5.7
BS5	57°33.3993′N	175°48.9659′W	1953	11.65	46600	0.66	0.00	0.09	7.41	5.4
BS5.5	57°33.3993′N	175°48.9659′W	1953	24	96000	0.70	0.00	0.11	6.31	5.3
BS6	57°33.3993′N	175°48.9659′W	1953	89	357280	0.59	0.00	0.10	6.06	4
BS7	57°33.3993′N	175°48.9659′W	1953	200	858800	0.61	0.00	0.10	6.17	2.5
BS8	57°33.3993′N	175°48.9659′W	1953	404	1618440	0.60	0.00	0.10	5.90	3.7
EQP 1 SEDA	01°48.2091'N	086°11.3787'W	2885	0.05	1351	0.59	27.64	0.09	6.46	9.4
EQP 1 SEDD	01°48.2091'N	086°11.3787'W	2885	10.18	275135	0.53	27.60	0.06	8.65	9.3
EQP 1 SEDE	01°48.2091'N	086°11.3787'W	2885	34	923513	0.44	24.87	0.07	6.49	7
EQP 1 SEDC	01°48.2091'N	086°11.3787'W	2885	7.21	194864	0.72	27.28	n/a	n/a	6.7
EQP 1 SEDB	01°48.2091'N	086°11.3787'W	2885	0.25	6757	0.76	27.71	0.10	7.98	6.3
EQP 8 SEDA	00°00.5291'N	147°47.4947'W	4336	0.05	10081	0.33	27.82	0.04	8.69	8.9
EQP 8 SEDB	00°00.5291'N	147°47.4947'W	4336	2.2	443548	0.28	27.89	0.02	14.12	8.0
EQP 8 SEDC	00°00.5291'N	147°47.4947'W	4336	26	5241935	0.23	27.74	0.00	n/a	5.4
IN1	16° 03.5577’ N	082° 05.6218’ E	895	4	40000	1.42	17.14	0.10	14.85	n/a
IN2	16° 03.5577’ N	082° 05.6218’ E	895	12	89999	1.26	13.79	0.10	13.21	n/a
IN3	16° 03.5577’ N	082° 05.6218’ E	895	21	212220	1.47	4.59	0.10	15.41	n/a
IN4	16° 03.5577’ N	082° 05.6218’ E	895	31	317775	1.70	0.04	0.10	17.44	n/a
IN5	16° 03.5577’ N	082° 05.6218’ E	895	40	423329	1.46	0.04	0.10	14.29	n/a
IN6	16° 03.5577’ N	082° 05.6218’ E	895	49	528884	1.72	0.00	0.11	15.74	n/a
IN7	16° 03.5577’ N	082° 05.6218’ E	895	59	633105	0.97	0.00	0.08	12.71	n/a

Extended Data Table 1: Environmental and sampling data collected for each of the four sampling location.

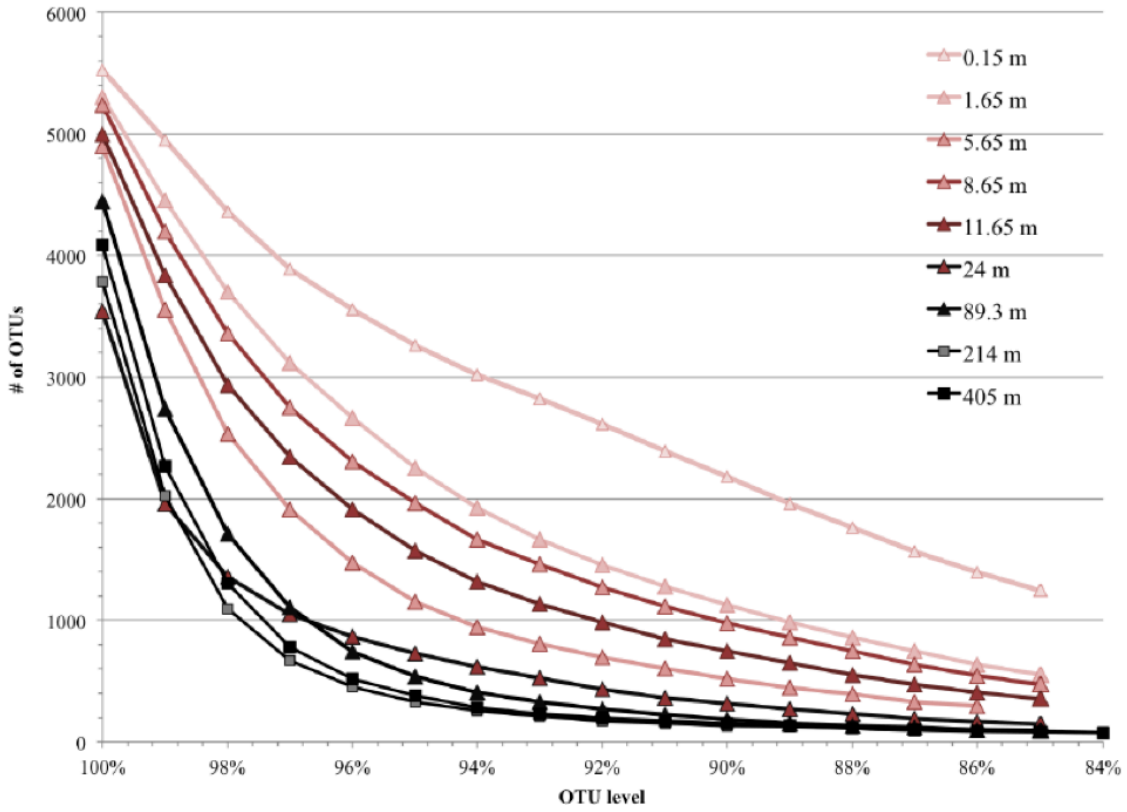

Extended Data Figure 1: Lineage through time (LTT) plot for the Bering Sea site U1343. The x-axis indicates clustering level (0-18%) and the y-axis indicates the number of OTUs generated. Trend was replicated at the remaining three sites (EQP1, EQP8 and NGHP-1-14) (data not shown).

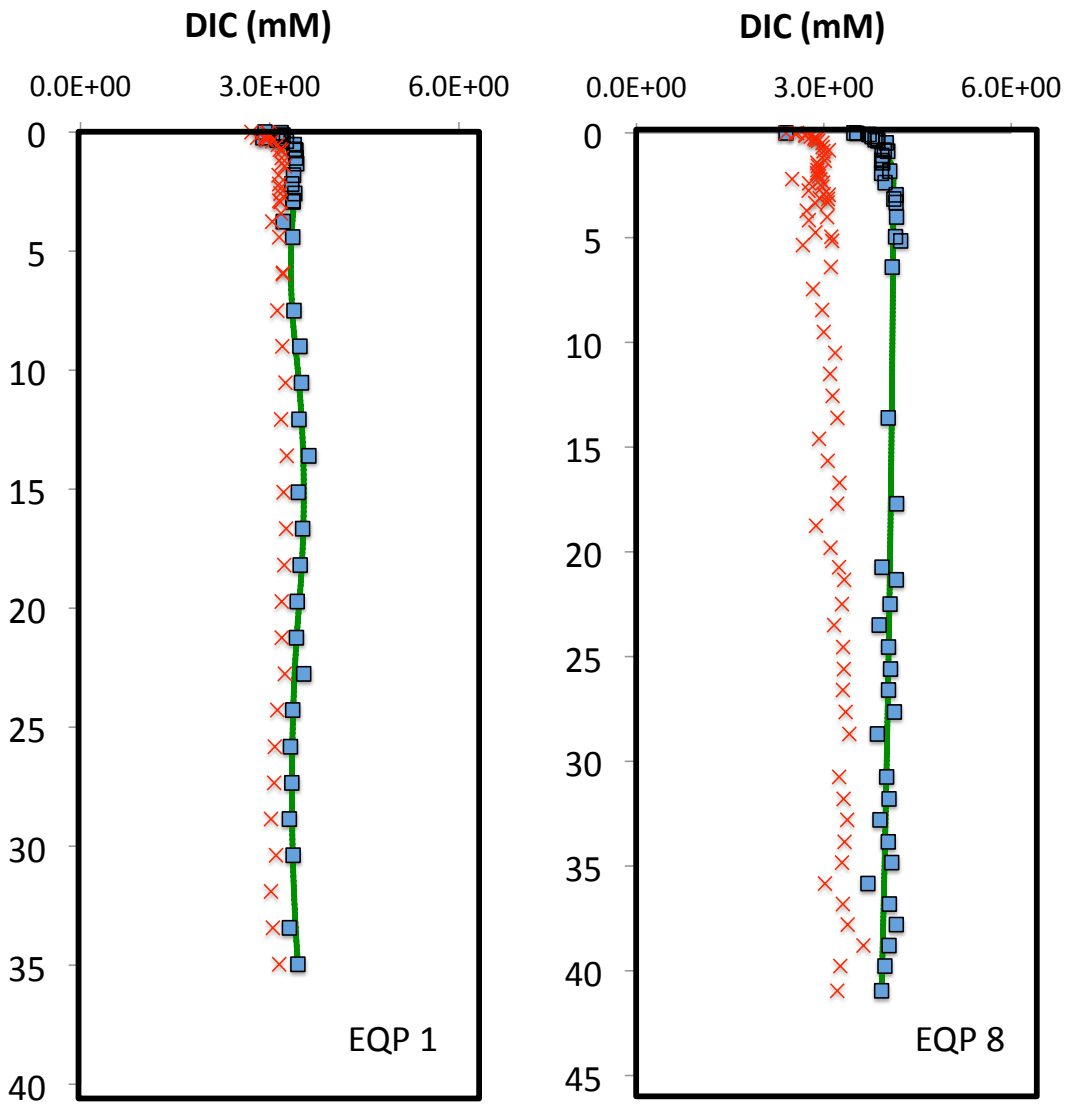

Extended Data Figure 2: Measured shipboard DIC (red stars) and corrected DIC (blue squares) for sites EQP1 and EQP8.

Extended Data Figure 3: Measured ammonium and DIC from Bering Sea site U1343. Each color circle represents a sample from one of the following three holes drilled: U1343A (Black), U1343B (Red) and U1343E (Blue). DIC and NH_4 Plots are from IODP expedition 323 sites U1343 preliminary report.

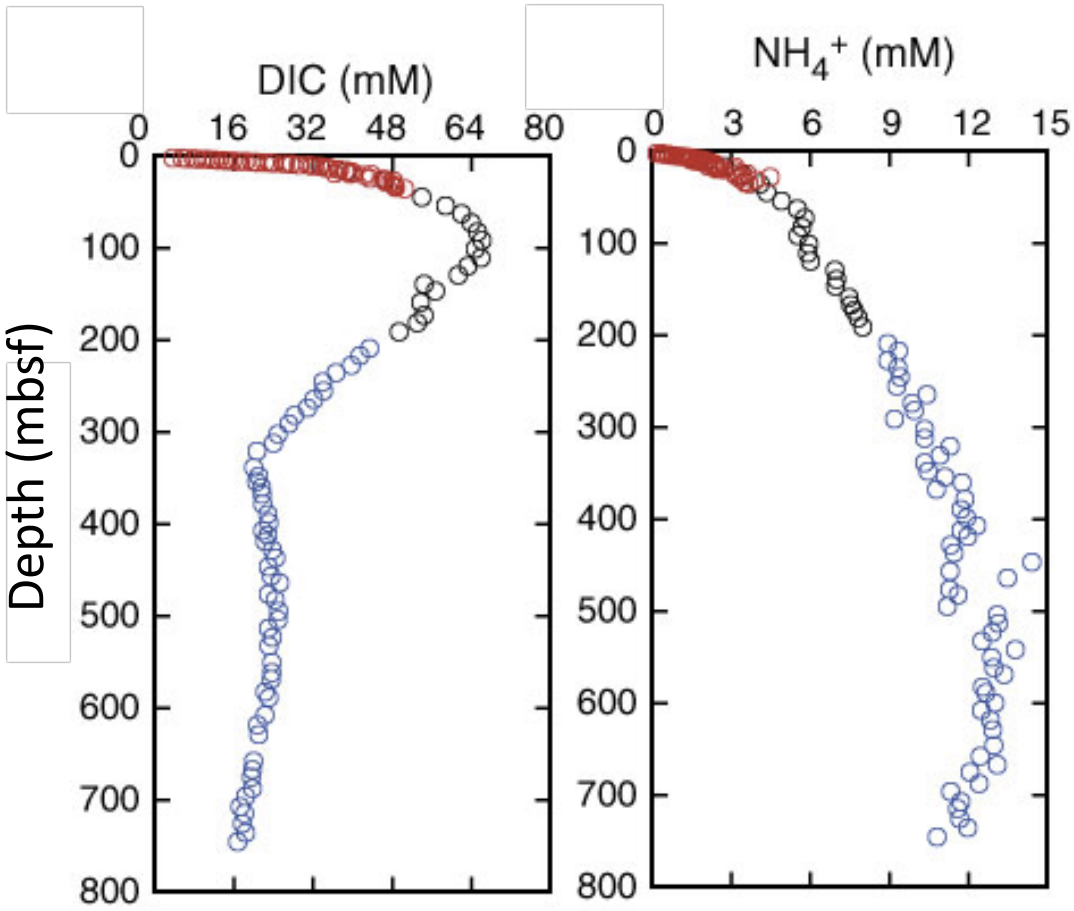

BIBLIOGRAPHY

D'Hondt, S., Jorgensen, B. B., Miller, D. J., Batzke, A., Blake, R., Cragg, B. A., . . . Acosta, J. L. S. (2004). Distributions of Microbial Activities in Deep Subseafloor Sediments. *Science, 306*(5705), 2216-2221. doi: 10.1126/science.1101155

Expedition 323 Scientists. (2010). Bering Sea paleoceanography: Pliocene–Pleistocene paleoceanography and climate history of the Bering Sea. *IODP preliminary report 323*. doi: doi:10.2204/iodp.sp.323.2009

Gieskes, J. M., Gamo, T., & Brumsack, H. (1991). Chemical methods for interstitial water analysis aboard JOIDES Resolution. *ODP Technical Note, 15*. doi: http://wwwodp.tamu.edu/publications/tnotes/tn15/ f_chem1.htm

Hamady, M., & Knight, R. (2009). Microbial community profiling for human microbiome projects: Tools, techniques, and challenges. *Genome Research, 19*, 1141-1152.

Jorgensen, B. B. (1978). A comparison of methods for the quantification of bacterial sulfate reduction in coastal marine sediments. *Geomicrobiology Journal, 1*(1), 49-64. doi: 10.1080/01490457809377723

Middelburg, J. J. (1989). A simple rate model for organic matter decomposition in marine sediments. *Geochimica et Cosmochimica Acta, 53*(7), 1577-1581. doi: http://dx.doi.org/10.1016/0016-7037(89)90239-1

Petrosino, J. F., Highlander, S., Luna, R. A., Gibbs, R. A., & Versalovic, J. (2009). Metagenomic pyrosequencing and microbial identification. *Clinical Chemistry, 55*, 856-866.

Westrich, J. T., & Berner, R. A. (1984). The role of sedimentary organic matter in bacterial sulfate reduction: The G model tested. *Liminology and Oceanography, 29*(2), 236-249.